This article has been accepted for publication in IEEE Transactions on Intelligent Vehicles. This is the author's version which has not been fully edited and content may change prior to final publication. Citation information: DOI 10.1109/TIV.2023.3337863

IEEE Transactions on Intelligent Vehicles, Available online 30 November 2023
DOI:10.1109/TIV.2023.3337863

Neural Network Observer based LPV Fault Tolerant Control of a Flying-wing Aircraft

Shiqian Liu, *Member, IEEE*, Weizhi Lyv, Congjie Yang, Feiyue Wang, *Fellow IEEE*, James F. Whidborne, *Senior Member, IEEE*

***Abstract*—For the problem of fault tolerant trajectory tracking control for a large Flying-Wing (FW) aircraft with Linear Parameter-Varying (LPV) model, a gain scheduled H_∞ controller is designed by dynamic output feedback. Robust synthesis of this gain scheduled H_∞ control is carried out by an affine Parameter Dependent Lyapunov Function (PDLF). The problem of trajectory tracking control for the LPV plant is transformed into solving an infinite number of linear matrix inequalities by the PDLF design, and the linear matrix inequalities are solved by convex optimization techniques. To overcome model uncertainties due to linearization and external disturbances, a radial basis function neural network disturbance observer is proposed, and to estimate actuator faults, an LPV fault estimator is designed. Furthermore, a composite controller is proposed to realize fault tolerant trajectory tracking control, which combines the LPV control with the fault estimator and disturbance observer, as well as an active-set based control allocation to avoiding actuator saturation. The approach is tested by simulation of two scenarios that show responses of the altitude, speed and heading angle to (i) unknown disturbances and (ii) actuator faults. The results show that the proposed neural network observer based LPV control has better performances for both disturbance rejecting and fault-tolerant trajectory tracking.**

***Index Terms*—Flying-wing aircraft; linear parameter-varying system; neural network; disturbance observer; fault tolerant control**

I. Introduction

THE flying-wing aircraft configuration has been proposed as a creative design for next generation aircraft [1]. Compared to the conventional configuration, the flying-wing has potential to meet future needs because of its capabilities for lower fuel consumption, smaller noise, carbon emission reduction and broader passenger cabin. Modeling and control methods of flying-wing aircrafts have been actively studied recent years [1, 2]. However, since there is no tail wing, there is a short pitch motion arm such that pitch balance of the airplane is very hard with potential for lose of control in landing; yaw control is also difficult[3]. Therefore, the question of how to control flying-wing aircraft is a particular challenge [4]. A feedback flight controller is required is to reduce pilot workload, particularly during abnormal conditions.

Because the aircraft nonlinear dynamics are changing with the flight conditions, gain-scheduling is a common appraoch. Although this is easily implemented in the engineering applications, it does not guarantee the overall closed-loop system robustness and nominal stability. A more systematic approach to deal with system uncertainty and nonlinearity is Linear Parameter-Varying (LPV) control [5, 6]. For example, Atoui *et al*. proposed LPV-based autonomous vehicle lateral controllers [5]. Damon proposed a Luenberger LPV observer to estimate lateral motorcycle dynamics and the rider action [6]. To realize a lane keeping system, Quan *et al.* proposed LPV model based gain-scheduling control with parameter reduction[7]. Liu and Sang studied a polytopic model for robust model predictive control of an airship with winds and state time-delay [8]. Fleps-Dezasse proposed an active fault tolerant LPV control to compensate for damper forces that may be lost after a failure [9]. It has been shown that stability and robustness of the closed-loop system is theoretically guaranteed by the LPV controllers[10].

It is known that the control performance of gain scheduling depends heavily on an accurate model. But flying-wing aircrafts are subject to a varying center of gravity, unknown faults, and other uncertainties. Furthermore, due to the short moment arm, they are more sensitive to center of gravity changes and to turbulence and gusts [4].

Robust control techniques, especially H_∞, have been proposed to handle such external disturbances and uncertainties. There are two well-known gain-scheduled H_∞ control method, this being the Single Quadratic Lyapunov Function (SQLF) [11] and the Parameter-Dependent Lyapunov Function (PDLF) [12, 13]. Compare with the SQLF design, the PDLF method is less conservative when

Manuscript received July 26, 2023;

This work was supported by the National Natural Science Foundation of China (52272400,10577012), and Shanghai Science and Technology Innovation Center for Systems Engineering of Commercial Aircraft Collaboration Fund (CASEF-M07)

S.Q. Liu, W.Z. Lyv, and C.J. Yang is with school of Aeronautics and Astronautics, Shanghai Jiao Tong University, Shanghai, 200240, China (e-mail:{liushiqian, weizhi_lyu, a15167773666}@sjtu.edu.cn)

F.Y.Wang, is withThe State Key Laboratory for Management and Control of Complex Systems, Institute of Automation, Chinese Academy of Sciences, Beijing 100190, China, (e-mail: feiyue.wang@ia.ac.cn)

J.F.Whidborne is with school of Aerospace, Transport and Manufacturing, Cranfield University, Cranfield MK43 0AL, UK(e-mail:j.f.whidborne@cranfield.ac.uk)

This article has been accepted for publication in IEEE Transactions on Intelligent Vehicles. This is the author's version which has not been fully edited and content may change prior to final publication. Citation information: DOI 10.1109/TIV.2023.3337863

the parameters are changing slowly [14, 15], hence the PDLF based LPV design is applied for flight control of the flying-wing aircraft.

The aim here is implement fault-tolerant trajectory tracking control for the FW aircraft under gust disturbances and unknown actuator faults, and so reduce gust and fault sensitiveness for the FW aircraft in a complex operation environment. This paper advocates a composite Fault Tolerant Trajectory Tracking Control (FTTTC) by using Neural Networks Disturbance Observer (NNs-DO) combined with a fault estimator.

NNs-DO has been used to estimate unknown bounded disturbances in the control process [16 17], and the control system can actively compensate for them. The advantage of the Disturbance observer based Control (DOBC) is that the original performances by baseline control are preserved and the observable disturbances are compensated without resorting to different control strategies [18]. Li et al. proposed an adaptive neural network output feedback optimized control design for a class of strict-feedback nonlinear systems that contain unknown internal dynamics and the states that are not measurable by means of barrier Lyapunov functions [19].

Hence, an NNs-DO based PDLF controller is proposed to fault tolerant control a flying-wing aircraft. This method is used to design the NNs observers to observe disturbances and estimate the actuator faults, and to integrate the faults and disturbance information into the LPV control scheme to reduce their influences. The main contributions of this study are listed as follows.

1) The LPV system of the flying-wing aircraft, under unknown disturbance and actuator faults, is robustly stabilized using the NNs-DO-PDLF LPV fault control. An H_∞ index is included in the NNs-DO-PDLF LPV design to reject environment disturbances. The FTTTC design problem of the LPV system with the H_∞ index and wind disturbances can be interpreted as an affine **parameter dependent Lyapunov function**. Compare to **a single quadratic Lyapunov function (SQLF) design proposed in [16], the PDLF method can reduce the conservatism of the designed LPV controller.**

2) **An RBF-NN disturbance observer is proposed in order to approximate model uncertainties and reject external disturbances**. Unlike **[16, 17], the RBF-NN is introduced into the DO, thus the disturbance observer improves adaptiveness and precision by the RBF neural-network approximation.** Meanwhile, An LPV fault estimator is proposed to compensate the influence of unknown actuator faults.

3) The flying-wing aircraft has fifteen control surfaces and three thrusters (see Fig.1). Hence a further challenge is how to efficiently allocate these control effectors. **An active set based weight square least method is suggested for this problem**. The fault tolerant control objective can be implemented in practice and actuator saturation is reduced.

The reminder of this paper is organized as follows. In Section II, an LPV dynamics model of a flying-wing aircraft is established. Section III proposes a NNs-DO PDLF based fault tolerant trajectory tracking control design. Section IV presents the simulation results as well as the discussions on the proposed method. Finally, the conclusion is drawn in Section V.

II. Dynamics Modeling

A. dynamics modeling of flying-wing aircrafts

The flying-wing aircraft configuration is shown in Fig.1, whose wing span 80m and length is 50.8m, and there are fifteen flaps for control, and it is assumed that the body is rigid. By using the Jacobian linearizing method a linear time invariant model [2] and the associated LPV model can be obtained.

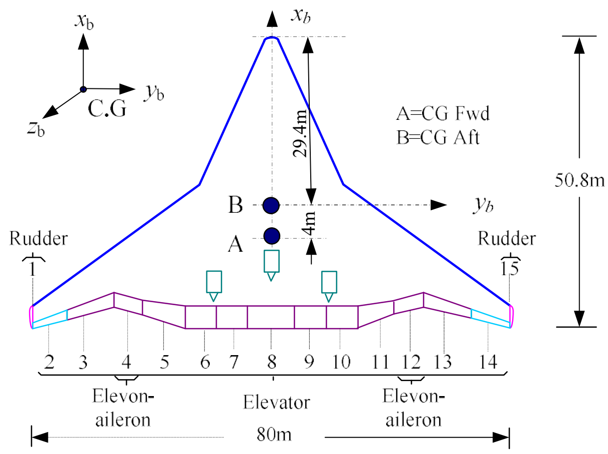

Fig. 1. Basic structure and control surfaces of a flying-wing aircraft

The LPV model is given by

$$\begin{cases} \dot{x}(t) = A(\rho)x(t) + B(\rho)u(t) \\ y(t) = C(\rho)x(t) + D(\rho)u(t) \end{cases}, \quad (1)$$

where $A(\cdot)$, $B(\cdot)$, $C(\cdot)$, and $D(\cdot)$ are given functions of scheduled parameters of ρ, $\rho = [\rho_1(t) \quad \rho_2(t) \quad \cdots \quad \rho_n(t)]^{\mathrm{T}}$ is scheduled parameters meeting $\rho_i(t) \in [\underline{\rho}_i, \bar{\rho}_i]$, $\underline{\rho}_i$, $\bar{\rho}_i$ denote upper and downer bound of ρ_i, i=1, 2, …, n. $x(t) \in \mathbb{R}^p$ is the state vector, $u(t) \in \mathbb{R}^{m_2}$ is the control input vector, $y(t) \in \mathbb{R}^{q_2}$ is the measurement output vector.

Since gust disturbances and faults often occur during flight for the FW aircraft, then the aircraft LPV model with disturbances and faults are described as

$$\begin{cases} \dot{x}(t) = A(\rho)x(t) + B_1(\rho)\omega(t) + \left(B_2(\rho)\left(u(t) + f_a(t)\right) + B_3 d(t)\right) \\ z(t) = C_1(\rho)x(t) + D_{11}(\rho)\omega(t) + D_{12}(\rho)u(t) \\ y(t) = C_2 x(t) + D_{21}(\rho)\omega(t) \end{cases} \quad (2)$$

where $A(\cdot)$, $B_1(\cdot)$, $B_2(\cdot)$, $C_1(\cdot)$, $D_{11}(\cdot)$, $D_{12}(\cdot)$ and $D_{21}(\cdot)$ are given functions of ρ. $\omega(t) \in \mathbb{R}^q$ is the L_2-norm bounded input disturbance, $d(t) \in \mathbb{R}^{m_3}$ denotes the unknown bounded disturbance, B_3 is effective matrix of the

This article has been accepted for publication in IEEE Transactions on Intelligent Vehicles. This is the author's version which has not been fully edited and content may change prior to final publication. Citation information: DOI 10.1109/TIV.2023.3337863

disturbance, $f_a(t)$ is actuator fault with bounded rate. $z(t)\in\mathbb{R}^{q_1}$ is the controlled variable or error vector.

To simplify the model and reduce computing load, assume that (B_2, C_2, D_{12}, D_{21}) are parameter independent, ($A(\rho)$, B_2) is quadratically stabilizable, and ($A(\rho)$, C_2) is detectable over the parameter space Θ. Then the model (2) is rewritten as

$$\begin{cases}\dot{x}(t)=A(\rho)x(t)+B_1(\rho)\omega(t)+B_2\left(u(t)+f_a(t)\right)+B_3d(t)\\ z(t)=C_1(\rho)x(t)+D_{11}(\rho)\omega(t)+D_{12}u(t)\\ y(t)=C_2x(t)+D_{21}\omega(t)\end{cases} \tag{3}$$

Set $B_3=B_2$ to match the disturbances from the control inputs, and the external disturbance can be generated by

$$\begin{cases}\dot{\xi}(t)=W_d\xi(t)\\ d(t)=V_d\xi(t)\end{cases} \tag{4}$$

where ξ is internal auxiliary variable, W_d and V_d are known suitable dimensional matrices. A PDLF based nominal controller is designed for the affine system (3),

$$\begin{cases}\dot{x}_k(t)=A_k(\rho,\dot{\rho})x_k(t)+B_k(\rho)y(t)\\ u_{LPV}(t)=C_k(\rho)x_k(t)+D_k(\rho)y(t)\end{cases} \tag{5a}$$

and

$$K(\rho)=\begin{pmatrix}A_k(\rho,\dot{\rho}) & B_k(\rho)\\ C_k(\rho) & D_k(\rho)\end{pmatrix}=\sum_{i=1}^{r}\alpha_iK_i\ ,K_i=\begin{pmatrix}A_{k_i} & B_{k_i}\\ C_{k_i} & D_{k_i}\end{pmatrix}, \tag{5b}$$

where $x_k(t)$ denotes the controller state, and A_k, B_k, C_k, D_k denote the controller gain matrices.

Denote $x_{cl}^T=\begin{bmatrix}x^T & x_k^T\end{bmatrix}$, if the disturbance $d(t)$ and faults $f_a(t)$ are neglected, then the closed-loop system, (2) and (5), is presented as follows,

$$\begin{bmatrix}\dot{x}_{cl}\\ z\end{bmatrix}=\begin{bmatrix}A_{cl}(\rho) & B_{1_{cl}}(\rho)\\ C_{1_{cl}}(\rho) & D_{11_{cl}}(\rho)\end{bmatrix}\begin{bmatrix}x_{cl}\\ \omega\end{bmatrix} \tag{6}$$

where

$$A_{cl}(\rho,\dot{\rho})=\begin{bmatrix}A(\rho)+B_2D_k(\rho)C_2 & B_2C_k(\rho)\\ B_k(\rho)C_2 & A_k(\rho,\dot{\rho})\end{bmatrix}=\sum_{i=1}^{r}\alpha_i\hat{A}_{cl_i}\ ,$$

$$B_{1_{cl}}(\rho)=\begin{bmatrix}B_1(\rho)+B_2D_k(\rho)D_{21}\\ B_k(\rho)D_{21}\end{bmatrix}=\sum_{i=1}^{r}\alpha_i\hat{B}_{cl_i}\ ,$$

$$C_{1_{cl}}(\rho)=\begin{bmatrix}C_1(\rho)+D_{12}D_k(\rho)C_2 & D_{12}C_k(\rho)\end{bmatrix}=\sum_{i=1}^{r}\alpha_i\hat{C}_{cl_i}\ ,$$

$$\hat{A}_{cl_i}=\begin{bmatrix}\tilde{A}_i+B_2\tilde{D}_{k_i}C_2 & B_2\tilde{C}_{k_i}\\ \tilde{B}_{k_i}C_2 & \tilde{A}_{k_i}\end{bmatrix},\ \hat{B}_{cl_i}=\begin{bmatrix}\tilde{B}_{1_i}+B_2\tilde{D}_{k_i}D_{21}\\ \tilde{B}_{k_i}D_{21}\end{bmatrix},$$

$$\hat{C}_{cl_i}=\begin{bmatrix}\tilde{C}_{1_i}+D_{12}\tilde{D}_{k_i}C_2 & D_{12}\tilde{C}_{k_i}\end{bmatrix},$$
$$D_{11_{cl}}(\rho)=D_{11}(\rho)+D_{12}D_k(\rho)D_{21}, \tag{7}$$

B. Problem formulation

To solve bounded disturbances and unknown faults, we are now ready to present the fault tolerant trajectory tracking control problem: Find an LPV fault tolerant control such that the closed-loop LPV system, (2) and (5), meets:

(a) robust stablity under conditions of bounded disturbances d and unknown faults f_a.

(b) rejection disturbance ω with H_∞ index so that

$$\|z(t)\|_{\ell_2}<\gamma\|\omega(t)\|_2 \tag{8}$$

for all nonzero $\omega(t)\in\ell_2[0,\infty)$, and

$$\|z(t)\|_{\ell_2}=\left[\int_0^\infty z^T(t)z(t)\mathrm{d}t\right]^{1/2}, \tag{9}$$

where γ is a given positive H_∞ index, $\|\cdot\|_{\ell_2}$ denotes L_2- norm operator.

III. Fault Tolerant Trajectory Tracking Control design

A. Control synthesis based on PDLF

The objective is to derive sufficient conditions driving the closed-loop system (6) meeting requirements of (a) and (b). First recall the definition of the asymptotically state invariant ellipsoids.

Lemma 1 [15] A given symmetric matrix polytope, $N(\rho)\in\mathbb{R}^{p\times p}$, for which $N(\rho)=\sum_{i=1}^{r}\alpha_iN_i$, meets $N(\rho)<0$ for $\forall\rho\in\Theta$, if and only if $N_i<0$, i = 1,2,…,m, where α_i is calculated by using (19) and (20)(defined later in this subsection), where $\Theta=\left[\underline{\rho}_1,\overline{\rho}_1\right]\times\left[\underline{\rho}_2,\overline{\rho}_2\right]\times\cdots\times\left[\underline{\rho}_n,\overline{\rho}_n\right]$, $\underline{\rho}_i$ and $\overline{\rho}_i$ denote the upper and lower bound of ρ_i respectively. n is the total number of $\rho(t)$.

The system state matrix $A(\rho)$, $B_1(\rho)$, $C_1(\rho)$ and $D_{11}(\rho)$ in (3) can be written as a convex combination of the matrix vertex, i.e.,

$$\begin{pmatrix}A(\rho) & B_1(\rho) & B_2\\ C_1(\rho) & D_{11}(\rho) & D_{12}\\ C_2 & D_{21} & 0\end{pmatrix}=\sum_{i=1}^{r}\alpha_i\begin{pmatrix}\tilde{A}_i & \tilde{B}_{1_i} & B_2\\ \tilde{C}_{1_i} & \tilde{D}_{11_i} & D_{12}\\ C_2 & D_{21} & 0\end{pmatrix} \tag{10}$$

where r = 2^n, $\tilde{A}_i$, $\tilde{B}_{1_i}$, $\tilde{C}_{1_i}$ and $\tilde{D}_{11_i}$ are the associated matrices at each vertex. By expanding the bounded real lemma [20] to LPV systems, we get the following conclusion; if there exists a positive definite symmetric matrix P such that

$$\begin{pmatrix}A^T(\rho)P+PA(\rho) & PB(\rho) & C^T(\rho)\\ B^T(\rho)P & -\gamma I & D^T(\rho)\\ C(\rho) & D(\rho) & -\gamma I\end{pmatrix}<0 \tag{11}$$

holds for all admissible parameter trajectories, then the system (1) is quadratic stable and guarantees the requirement $\|z(t)\|_{\ell_2}<\gamma\|\omega(t)\|_2$ [20].

Consider the LPV system $\dot{x}=A(\rho)x$, by using Lyapunov stability theory it can be seen that the LPV system is parameter-dependent stable if and only if there exists a positive definite symmetric matrix $P(\rho)=P^T(\rho)$ such that

$$A^T(\rho)P(\rho)+P(\rho)A(\rho)+\dot{P}(\rho)<0,\forall(\rho,\dot{\rho})\in\Theta\times\Phi \tag{12}$$

where

$$\Phi=\left[\underline{\theta}_1,\overline{\theta}_1\right]\times\left[\underline{\theta}_2,\overline{\theta}_2\right]\times\cdots\left[\underline{\theta}_n,\overline{\theta}_n\right], \tag{13}$$

$\underline{\theta}_i$ and $\overline{\theta}_i$ denote the upper and lower bound of θ_i meeting $\theta_i=\dot{\rho}_i$, respectively. $P(\rho)$ and $\dot{P}(\rho)$ depend affinely on the parameters ρ as[12],

$$P(\rho)=P_0+\rho_1P_1+\cdots+\rho_nP_n=\alpha_1\tilde{P}_1+\alpha_2\tilde{P}_2+\cdots+\alpha_r\tilde{P}_r,\ r=2^n, \tag{14}$$

$$\dot{P}(\rho)=\dot{\rho}_1P_1+\cdots+\dot{\rho}_nP_n=\beta_1\hat{P}_1+\beta_2\hat{P}_2+\cdots+\beta_r\hat{P}_r. \tag{15}$$

where $\tilde{P}_i$ and $\hat{P}_i$ are intermediate variants. Substituting (10) , (14) and (15) into (12) yields

$$\sum_{i=1}^{r}\sum_{k=1}^{r}\alpha_i\alpha_i\beta_k\left(\tilde{A}_i^T\tilde{P}_i+\tilde{P}_i\tilde{A}_i+\hat{P}_k\right)+2\sum_{i=1}^{r-1}\sum_{j=i+1}^{r}\sum_{k=1}^{r}\alpha_i\alpha_j\beta_k\left(\frac{1}{2}\left(\tilde{A}_i^T\tilde{P}_j+\tilde{P}_j\tilde{A}_i+\tilde{A}_j^T\tilde{P}_i+\tilde{P}_i\tilde{A}_j+2\hat{P}_k\right)\right)<0$$

$$,\forall(\rho,\dot{\rho})\in\Theta\times\Phi \tag{16}$$

where

$$\alpha_i\alpha_i\beta_k\in[0,1],\alpha_i\alpha_j\beta_k\in[0,0.5],\ \sum_{i=1}^{r}\alpha_i=1,\sum_{i=1}^{r}\beta_i=1, \tag{17}$$

$$\sum_{i=1}^{r}\sum_{k=1}^{r}\alpha_i\alpha_i\beta_k+2\sum_{i=1}^{r-1}\sum_{j=i+1}^{r}\sum_{k=1}^{r}\alpha_i\alpha_j\beta_k=1. \tag{18}$$

To calculate α_i or β_i , the normalized co-ordinate is computed as

$$\alpha_{\rho_i}=\frac{\overline{\rho}_i-\rho_i(t)}{\overline{\rho}_i-\underline{\rho}_i},\ i=1,2,\cdots,n \tag{19}$$

Then the associated polytopic co-ordinates for each vertex are computed by[21].

$$\alpha_j=\prod_{i=1}^{n}\tilde{\alpha}_{\rho_i},\tilde{\alpha}_{\rho_i}=\begin{cases}\alpha_{\rho_i}, & \text{if } \underline{\rho}_i \text{ is a co-ordinate of } \Theta_j\\ 1-\alpha_{\rho_i}, & \text{if } \overline{\rho}_i \text{ is a co-ordinate of } \Theta_j\end{cases},$$

$$j=1,2,\ldots,r, \tag{20}$$

According to Lemma 1, if positive definite symmetric matrices $\tilde{P}_i$ are done at all vertices, then the inequality of (16) is solved. Therefore, if the existence of a positive definite matrix $P_i>0$, i = 1, 2,…, r satisfies the following LMIs

$$\tilde{A}_i^T\tilde{P}_i+\tilde{P}_i\tilde{A}_i+\hat{P}_k<0,\tilde{P}_i>0 \tag{21}$$

$$\tilde{A}_i^T\tilde{P}_j+\tilde{P}_j\tilde{A}_i+\tilde{A}_j^T\tilde{P}_i+\tilde{P}_i\tilde{A}_j+2\hat{P}_k<0 \tag{22}$$

$$(i,k=1,2,\ldots,r \text{ and } 1\le i<j\le r),$$

then the system $\dot{x}=A(\rho)x$ is parameter-dependent stable.

By using the PDLF of $V(x)=x^TP(\rho)x$, we get that an LPV controller $K(\boldsymbol{\rho})$ stabilizes the closed-loop system (6), and ensures the H_∞ index $\|z(t)\|_{\ell_2}<\gamma\|\omega(t)\|_2$ if and only if there exists $P(\rho)=P^T(\rho)$ satisfying

$$P(\rho)>0,\frac{d}{dt}\left(x^TP(\rho)x\right)+z^Tz-\gamma\omega^T\omega<0,$$

$$\forall(\rho,\dot{\rho})\in\Theta\times\Phi, \tag{23}$$

then a scaled bounded real lemma inequality is got from inequality (23) [12]

$$\begin{bmatrix}\tilde{A}_{cl}+\dot{P}(\rho) & P(\rho)B_{1_{cl}}(\rho) & C_{1_{cl}}^T(\rho)\\ * & -\gamma I & D_{11_{cl}}^T(\rho)\\ * & * & -\gamma I\end{bmatrix}<0 \tag{24}$$

where $\tilde{A}_{cl}=A_{cl}^T(\rho,\dot{\rho})P(\rho)+P(\rho)A_{cl}(\rho,\dot{\rho})$, * denotes a symmetric matrix block,

Since the matrices of $P(\rho),A_k(\rho,\dot{\rho}),B_k(\rho),C_k(\rho),D_k(\rho)$, $A_{cl}(\rho,\dot{\rho}),B_{1_{cl}}(\rho),C_{1_{cl}}(\rho),D_{11_{cl}}(\rho)$ do not depend affinely on parameters ρ, for facilitating the LPV control design, the intermediate variables $\tilde{A}_k(\rho)$, $\tilde{B}_k(\rho)$, $\tilde{C}_k(\rho)$ and $D_k(\rho)$ are set to depend affinely on the parameters ρ as following [12]

$$\begin{aligned}\tilde{A}_k(\rho)&=\tilde{A}_{k_0}+\rho_1\tilde{A}_{k_1}+\cdots+\rho_n\tilde{A}_{k_n}=\alpha_1\hat{A}_{k_1}+\alpha_2\hat{A}_{k_2}+\cdots+\alpha_r\hat{A}_{k_r}\\ \tilde{B}_k(\rho)&=\tilde{B}_{k_0}+\rho_1\tilde{B}_{k_1}+\cdots+\rho_n\tilde{B}_{k_n}=\alpha_1\hat{B}_{k_1}+\alpha_2\hat{B}_{k_2}+\cdots+\alpha_r\hat{B}_{k_r}\\ \tilde{C}_k(\rho)&=\tilde{C}_{k_0}+\rho_1\tilde{C}_{k_1}+\cdots+\rho_n\tilde{C}_{k_n}=\alpha_1\hat{C}_{k_1}+\alpha_2\hat{C}_{k_2}+\cdots+\alpha_r\hat{C}_{k_r}\\ D_k(\rho)&=\tilde{D}_{k_0}+\rho_1\tilde{D}_{k_1}+\cdots+\rho_n\tilde{D}_{k_n}=\alpha_1\hat{D}_{k_1}+\alpha_2\hat{D}_{k_2}+\cdots+\alpha_r\hat{D}_{k_r}\end{aligned}$$

$$, \tag{25}$$

then we obtain

$$\begin{aligned}A_k(\rho,\dot{\rho})=N^{-1}(\rho)\Big(&R(\rho)\dot{S}(\rho)+N(\rho)\dot{M}^T(\rho)+\tilde{A}_k(\rho)\\ &-R(\rho)\left(A(\rho)-B_2D_k(\rho)C_2\right)S(\rho)\\ &-\tilde{B}_k(\rho)C_2S_k(\rho)-R(\rho)B_2\tilde{C}_k(\rho)\Big)M^{-T}(\rho)\end{aligned} \tag{26}$$

$$B_k(\rho)=N^{-1}(\rho)\left(\tilde{B}_k(\rho)-R(\rho)B_2D_k(\rho)\right),$$

$$C_k(\rho)=\left(\tilde{C}_k(\rho)-D_k(\rho)C_2S(\rho)\right)M^{-T}(\rho), \tag{27}$$

where

$$N(\rho)=-R(\rho)+S^{-1}(\rho),$$

$$\dot{N}(\rho)=-\dot{R}(\rho)-S^{-1}(\rho)\dot{S}(\rho)S^{-1}(\rho),M(\rho)=S(\rho),$$

$$\dot{M}(\rho)=\dot{S}(\rho). \tag{28}$$

The positive definite symmetric matrix pair of ($R(\rho)$, $S(\rho)$) comes from the parameter-dependent Lyapunov variable of $P(\rho)$ as

$$P(\rho)=\begin{bmatrix} R(\rho) & -\left(R(\rho)-S^{-1}(\rho)\right) \\ -\left(R(\rho)-S^{-1}(\rho)\right) & R(\rho)-S^{-1}(\rho) \end{bmatrix}$$

$$=\begin{bmatrix} I_p & R(\rho) \\ 0_{p\times p} & -\left(R(\rho)-S^{-1}(\rho)\right) \end{bmatrix}\begin{bmatrix} S(\rho) & I_p \\ S(\rho) & 0_{p\times p} \end{bmatrix}, \quad (29)$$

where $R(\rho)-S^{-1}(\rho)\geq 0$, and rank $\left(R(\rho)-S^{-1}(\rho)\right)\leq p$. Eqs(26)~(28) show that the controller matrices of $A_k(\rho,\dot{\rho})$, $B_k(\rho)$, $C_k(\rho)$ do not depend affinely on the scheduled parameters *ρ*. For convenience, denote ($R(\rho)$, $S(\rho)$) to depend affinely on the parameters *ρ* as

$$R(\rho)=R_0+\rho_1 R_1+\cdots+\rho_n R_n=\alpha_1\tilde{R}_1+\alpha_2\tilde{R}_2+\cdots+\alpha_r\tilde{R}_r ,$$
$$S(\rho)=S_0+\rho_1 S_1+\cdots+\rho_n S_n=\alpha_1\tilde{S}_1+\alpha_2\tilde{S}_2+\cdots+\alpha_r\tilde{S}_r , \quad (30)$$
$$\dot{R}(\rho)=\dot{\rho}_1 R_1+\cdots+\dot{\rho}_n R_n=\beta_1\hat{R}_1+\beta_2\hat{R}_2+\cdots+\beta_r\hat{R}_r ,$$
$$\dot{S}(\rho)=\dot{\rho}_1 S_1+\cdots+\dot{\rho}_n S_n=\beta_1\hat{S}_1+\beta_2\hat{S}_2+\cdots+\beta_r\hat{S}_r . \quad (31)$$

where R_i and S_i is mapped into $\hat{R}_j$ and $\hat{S}_j$ respectively as (14), j = 1, ... , r, i = 1, ... ,n. Substituting (14), (25)~(31) into (24) yields

$$\begin{bmatrix} \Lambda(R)+\dot{R}(\rho) & \tilde{A}_k(\rho)+A^T(\rho)+C_2^T D_k^T(\rho)B_2^T & R(\rho)B_1(\rho)+\tilde{B}_k(\rho)D_{21} & C_1^T(\rho)+C_2^T D_k^T(\rho)D_{12}^T \\ * & \Lambda(S)-\dot{S}(\rho) & B_1(\rho)+B_2D_k(\rho)D_{21} & S(\rho)C_1^T(\rho)+\tilde{C}_k^T(\rho)D_{12}^T \\ * & * & -\gamma I & D_{11}^T(\rho)+D_{21}^T D_k^T(\rho)D_{12}^T \\ * & * & * & -\gamma I \end{bmatrix}<0 \quad (32)$$

where

$$\Lambda(R)=R(\rho)A(\rho)+\tilde{B}_k(\rho)C_2+A^T(\rho)R(\rho)+C_2^T\tilde{B}_k^T(\rho) ,$$
$$\Lambda(S)=A(\rho)S(\rho)+B_2\tilde{C}_k(\rho)+S(\rho)A^T(\rho)+\tilde{C}_k^T(\rho)B_2^T .$$

Substituting (25), (30) and (31) into (32), we get [14]

$$\sum_{i=1}^{r}\sum_{k=1}^{r}\alpha_i\alpha_i\beta_k\left(\Psi_{cl_i}+\bar{Q}^T\tilde{K}_i^T\bar{P}_{cl}+\bar{P}_{cl}^T\tilde{K}_i\bar{Q}\right)$$
$$+2\sum_{i=1}^{r-1}\sum_{j=i+1}^{r}\sum_{k=1}^{r}\alpha_i\alpha_j\beta_k\left(\frac{1}{2}\left(\Psi_{cl_{ij}}+\bar{Q}^T\tilde{K}_i^T\bar{P}_{cl}+\bar{P}_{cl}^T\tilde{K}_i\bar{Q}+\Psi_{cl_{ji}}+\bar{Q}^T\tilde{K}_j^T\bar{P}_{cl}+\bar{P}_{cl}^T\tilde{K}_j\bar{Q}\right)\right)<0 \quad (33)$$

where

$$\Psi_{cl_{ij}}=\begin{bmatrix} \tilde{A}_i^T\tilde{R}_j+\tilde{R}_j\tilde{A}_i+\hat{R}_k & \tilde{A}_i & \tilde{R}_j\tilde{B}_{1_i} & \tilde{C}_{1_i}^T \\ * & \tilde{A}_iS_j+S_j\tilde{A}_i^T-\hat{S}_k & \tilde{B}_{1_i} & S_j\tilde{C}_{1_i}^T \\ * & * & -\gamma I & \tilde{D}_{11_i} \\ * & * & * & -\gamma I \end{bmatrix} \quad (34)$$

$$\bar{Q}=\begin{bmatrix} \bar{C} & \bar{D}_{21} & 0_{(p+q_2)\times q_1} \end{bmatrix}, \quad (35)$$

$$\bar{P}_{cl}=\begin{bmatrix} \bar{B}^T & 0_{(p+m_2)\times m_1} & \bar{D}_{12}^T \end{bmatrix}. \quad (36)$$

$$\tilde{B}=\begin{bmatrix} I & 0 \\ 0 & B_{2,sw} \end{bmatrix},\ \tilde{K}_i=\begin{pmatrix} \hat{A}_{k_i} & \hat{B}_{k_i} \\ \hat{C}_{k_i} & \hat{D}_{k_i} \end{pmatrix}. \quad (37)$$

By Lemma 1, the LMIs (33) are sufficiently validated at all vertices. If $\tilde{K}_i$ (i = 1, 2, …, r) has been obtained by the LMIs (33), then the dynamic controller of (5) can be computed on-line by using Eqs (26) ~ (28) with instantaneous measurement values of ρ and $\dot{\rho}$.

Remark 1 The parameter derivatives $\dot{\rho}$ are sometimes unavailable during flight [12]. To overcome this, $R(\rho)$ or $S(\rho)$ can be constrained to depend affinely on ρ. This yields

$$\dot{R}(\rho)S(\rho)+\dot{N}(\rho)M^T(\rho)=-\left(R(\rho)\dot{S}(\rho)+N(\rho)\dot{M}^T(\rho)\right)=0 \quad (38)$$

Then Eq.(26) is rewritten as

$$A_k(\rho,\dot{\rho})=N^{-1}(\rho)\left(\tilde{A}_k(\rho)-R(\rho)\left(A(\rho)-B_2D_k(\rho)C_2\right)S(\rho)-\tilde{B}_k(\rho)C_2S_k(\rho)-R(\rho)B_2\tilde{C}_k(\rho)\right)M^{-T}(\rho) . \quad (39)$$

B. DO and fault estimator based fault tolerant control

As disturbances and faults may occur at unknown time and intensity, an accurate model is impossible to achieve. Hence a disturbance observer and a fault one are introduced into LPV control. A DO-based FTC is proposed for this purpose. The disturbance observer and the fault estimator are designed to separately estimate the unknown observable disturbances and actuator faults.

Furthermore, considering some model uncertainties except for external disturbances, such as Jacobian linearization error, a radial basis function neural network (RBF-NN) is approximate to this model uncertainty. The structure of the RBF-NN is three layers, first is the input layer, the net input is $x_{NN}=\begin{bmatrix} e^T & \dot{e}^T \end{bmatrix}^T$, where $e=x-x_d$, $\dot{e}=\dot{x}-\dot{x}_d$, x_d denotes the desired state variant. Second is the hidden layer, each node performs a membership function, whose basis function is presented as following Gaussian function

$$h_j(x_{NN})=\exp\left(-\left\|x_{NN}-c_j\right\|^2/\left(2b_j^2\right)\right) \quad (40)$$

where b_j is the Gaussian function width, c_j is the centre value, j denotes the node number of the hidden layer. The third is the output layer, whose output is

This article has been accepted for publication in IEEE Transactions on Intelligent Vehicles. This is the author's version which has not been fully edited and content may change prior to final publication. Citation information: DOI 10.1109/TIV.2023.3337863

$$y_{NN} = W^T h\left(x_{NN}\right) \tag{41}$$

where W is the best weight vector, whose update law is

$$\dot{\hat{W}} = \gamma_W e^T h(x_{NN}) . \tag{42}$$

where γ_w denotes learn rate gain. The model error can be presented as

$$\Delta\Sigma = W^{*T} h\left(x_{NN}\right) + \varepsilon\left(x_{NN}\right) \tag{43}$$

where ε denotes approximation error, W^* is the optimal weight matrix.

Furthermore, a disturbance observer with an RBF neural-network approximation is designed to improve trajectory tracking precision [17].

$$\begin{cases} \dot{z}_d = (W_d - L_d(x)B_3V_d)\hat{\xi} \\ \quad - L_d(x)\left(A(\rho)x + B_2(\rho)u + \hat{W}^T h(x) + B_2(\rho)\hat{f}_a\right) \\ \hat{\xi} = z_d + L_d(x)x \\ \hat{d} = V_d\hat{\xi} \end{cases} \tag{44}$$

where $\hat{d}$ is disturbance estimation, z_d is the internal state, and $L_d(x)$ is the observer gains to be designed, $\hat{W}$ is the best estimation of the RBF-NN weight vector, $\hat{\xi}$ and $\hat{f}_a$ are estimation of ξ and fault f_a. The disturbance estimation error is denoted by $e_\xi = \xi - \hat{\xi}$, by Eqs (2)-(3) and Eq.(44) the derivative $\dot{e}_\xi$ is

$$\dot{e}_\xi(t) = \left(W_d - L_d(x)B_3V_d\right)e_\xi(t) - B_1(\rho)\omega . \tag{45}$$

where the term of $-B_1(\rho)\omega$ can be stabilized by the LPV controller.

Provided that the observer dynamics change fast relative to the disturbances, select the observer gain $L_d(x)$ is selected so that $W_d - L_d(x)B_3V_d$ is Hurwitz, then the disturbance estimation error, Eq. (45), is exponentially stable.

The fault diagnosis estimator is proposed as follows

$$\begin{cases} \hat{f}_a(t) = \zeta(t) + L_f(x)x(t) \\ \dot{\zeta}(t) = -L_f(x)B_2(\rho)\left(\zeta(t) + L_f(x)x(t)\right) \\ \quad - L_f(x)\left(A(\rho)x(t) + B_2(\rho)u(t) + B_3\hat{d}(t)\right) \end{cases} \tag{46}$$

where $\hat{f}_a(t)$ is the estimation of fault $f_a(t)$, $L_f(x)$ is the estimator gain and $\zeta(t)$ is the internal auxiliary variable. The fault estimation error is $e_f = f_a - \hat{f}_a$, by (2)-(3), (44) and Eq.(46) the derivative $\dot{e}_f$ is given as

$$\dot{e}_f(t) = \dot{f}_a - \dot{\hat{f}}_a = -L_f B_2 e_f(t) - B_3V_d e_\xi(t) - B_1\omega + \dot{f}_a(t) \tag{47}$$

Usually $f_a(t)$ persists only for a limited time, until the fault has been diagnosed and the system is reconfigured [22], so the fault derivative is assumed to be bounded. To this end, the composite fault tolerant controller with the dynamic output feedback (5) is proposed as

$$v(t) = u_{LPV}(t) + u_d(t) + u_f(t) \tag{48}$$

and

$$u_{LPV} = C_k(\rho)x_k(t) + D_k(\rho)y(t) , \tag{49}$$

$$u_d = K_d\hat{d} . \tag{50}$$

where

$$K_d = -B_2^+ B_3 . \tag{51}$$

$$u_f(t) = -\hat{f} \tag{52}$$

u_f is the fault tolerant control designed by the fault estimator, + denotes Moore-Penrose inversion. We attempt to find appropriate disturbance observer gain $L_d(x)$ and fault estimation gain $L_f(x)$ to construct a composite controller, thus the external disturbances can be reduced and faults is compensated, finally, the input of the LPV controller is reduced.

C. The FTTTC design

The controller structure including the longitude and lateral motions is proposed as in Fig.2,where e_{lon}=ref$_{lon}$−$[u, h]^T$, e_{lat}=ref$_{lat}$−$[v, \psi]^T$ y_{lon}=$[u,w,q,\theta,h]^T$, y_{lat}= $[v,p,r, \phi,\psi]^T$. x^T_{NNs}= $[x^T_{ref}, x^T, x^T_k]$,Zy$_{lon}$=$[Z_u,Z_h]$, Zy$_{lat}$=$[Z_v,Z_\psi]$, Z$_{\delta lon}$=$[Z_{\delta e},Z_{\delta p}]$, Z$_{\delta llat}$=$[Z_{\delta a},Z_{\delta r}]$. In this scheme the PDLF approach is applied to reduce the LPV design conservatism. The trajectory tracking task is implemented by the LPV controller with guarantee H_∞ index. Disturbance and actuator faults are estimated by the NN-DO and a fault estimator. Control allocation is used to realize virtual control by practical control surfaces. A pre-filter is introduced to suppress high frequency signal inputs. The next section will present the LPV controller design.

Lemma 2 [Finsler's lemma][23] the following statements are equivalent

(i) $$\exists\mu \in \mathbb{R} : \begin{cases} Q - \mu B^T B < 0 \\ Q - \mu C^T C < 0 \end{cases}, \tag{53}$$

and given the inequality

(ii) $$Q + B^T X^T C + CXB < 0 , \tag{54}$$

is solvable for $X \in \mathbb{R}^{n\times m}$ if and only if

$$B_\perp^T Q B_\perp < 0 , C_\perp^T Q C_\perp < 0 \tag{55}$$

where $Q \in \mathbb{R}^{m\times m}$ is a symmetric matrix. $B_\perp$ and $C_\perp$ are matrices whose columns from bases of the null spaces of B and C respectively.

This article has been accepted for publication in IEEE Transactions on Intelligent Vehicles. This is the author's version which has not been fully edited and content may change prior to final publication. Citation information: DOI 10.1109/TIV.2023.3337863

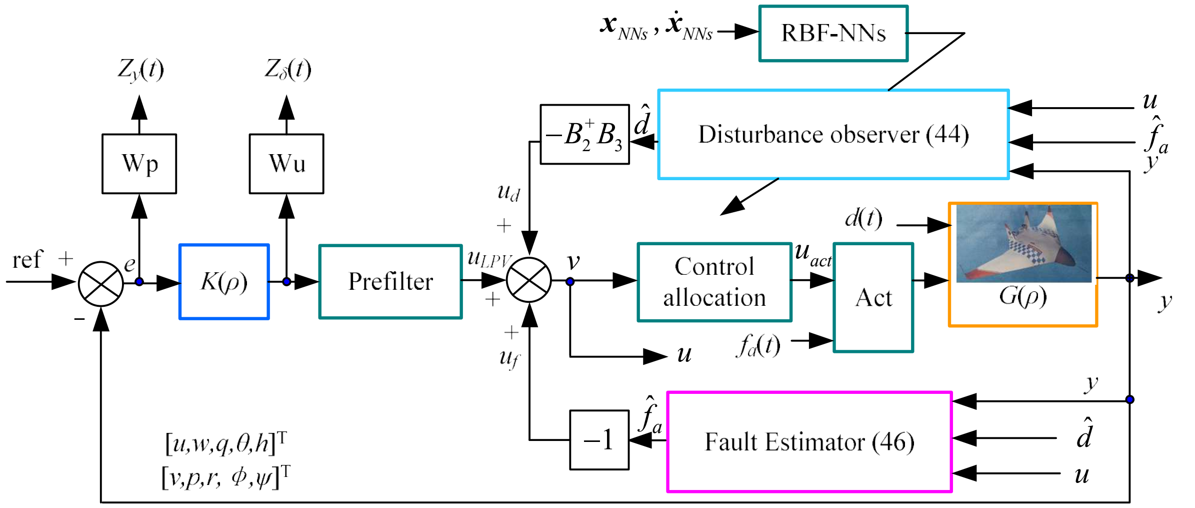

Fig.2 Block diagram of the designed fault tolerant trajectory tracking control

Lemma 3 [24] Consider the nonlinear system $\dot{x} = f(x,\varepsilon)$ is continuously differentiable and the Jacobian matrices satisfy $\left\|\frac{\partial f(x,\varepsilon)}{\partial x}\right\| \le \tau_1$ and $\left\|\frac{\partial f(x,\varepsilon)}{\partial \varepsilon}\right\| \le \tau_2 \|x\|$ for all $(x,\varepsilon)\in \Xi\times\Gamma$, $\Xi \triangleq \{x\in R^n \mid \|x\|<r\}$, $\varepsilon\in\Gamma\subset R$, Γ is real number subset. Let k,λ,r_0 be positive constant with $r_0 < r/k$ and define $\Xi_0 \triangleq \{x\in R^n \mid \|x\|<r_0\}$. Assume that the system trajectory meets $\|x\| < k\|x(0)\|e^{-\lambda t}, \forall x(0)\in\Xi_0, \varepsilon\in\Gamma, t\ge 0$. Then there is a function $V: \Xi_0\times\Gamma\to R$ such that the inequalities:

$$c_1\|x\|^2 \le V(x,\varepsilon) \le c_2\|x\|^2, \tag{56}$$

$$\frac{\partial V}{\partial x} f(x,\varepsilon) \le -c_3\|x\|^2. \tag{57}$$

$$\left\|\frac{\partial V}{\partial x}\right\| \le c_4\|x\|, \left\|\frac{\partial V}{\partial \varepsilon}\right\| \le c_5\|x\|^2 \tag{58}$$

hold, where c_i (i=1,2,..5) is positive constant. Moreover, if all the assumptions hold globally (in x), then $V(x,\varepsilon)$ is defined and meets the above conditions on $R\times\Gamma$.

Lemma 4 [26]. Assume that A1) $d(0)$=0; A2) $A(\rho), B_2(\rho), d, \partial d/\partial x$ are all continuously differentiable; A3) $\dot{x}(t)=A(\rho)x(t)+B_2(\rho)u(t)$ is exponentially stable. Provide that A1)~ A3) are met, then the closed-loop system (3), (44) and (46) under the proposed controller (5) with (48)~(52) is exponentially stable if the observer gain $L_d(x)$ is selected such that $\dot{e}_\xi(t)=(-\gamma_d L_d(x)B_3V_d)e_\xi(t)$ is exponentially stable for all $x \in B_r=\{x \mid \|x\|<r\}$, where γ_d is a given sufficiently large positive value.

By using Lemma 3 and 4, we can get following conclusion.

Theorem 1 The existence composite controller of (48)~(52), with a NN observer (44) and a fault estimator (46), assures the closed-loop system (2) and (5), satisfying desired performances of (*a*) and (*b*), if the observer gain $L_d(x)$ and $L_f(x)$ are appropriately determined such that $W_d - L_d(x)B_3V_d$ and $-L_f(x)B_2$ are Hurwitz respectively, and the following LMI conditions hold for a pair of positive definite symmetric matrices ($R(\rho), S(\rho)$)

$$\bar{N}_R{}^T \Xi_R \bar{N}_R < 0, \tag{59}$$

$$\bar{N}_S{}^T \Xi_S \bar{N}_S < 0 \tag{60}$$

$$\bar{N}_R{}^T \Xi_{\hat{R}} \bar{N}_R < 0 \tag{61}$$

$$\bar{N}_S{}^T \Xi_{\hat{S}} \bar{N}_S < 0 \tag{62}$$

$$\begin{pmatrix} R_i & I \\ I & S_i \end{pmatrix} > 0 \text{ , for } i = 1, \ldots, \text{r}. \tag{63}$$

$$\text{rank}\left(R(\rho) - S^{-1}(\rho)\right) \le p \tag{64}$$

where $\bar{N}_R = \begin{pmatrix} N_R & 0 \\ 0 & I \end{pmatrix}$, $\bar{N}_S = \begin{pmatrix} N_S & 0 \\ 0 & I \end{pmatrix}$, N_R and N_S denote bases of the null spaces of $[C_2, D_{21}]$ and $[B_2^T, D_{12}^T]$, respectively.

$$\Xi_R = \begin{bmatrix} \tilde{A}_i^T\tilde{R}_i + \tilde{R}_i\tilde{A}_i + \hat{R}_k & \tilde{R}_i\tilde{B}_{1_i} & \tilde{C}_{1_i}{}^T \\ * & -\gamma I & \tilde{D}_{1_i}^T \\ * & * & -\gamma I \end{bmatrix},$$

$$\Xi_S = \begin{bmatrix} \tilde{A}_i\tilde{S}_i + \tilde{S}_i\tilde{A}_i^T - \hat{S}_k & \tilde{S}_i\tilde{C}_{1_i}{}^T & \tilde{B}_{1_i} \\ * & -\gamma I & \tilde{D}_{11_i} \\ * & * & -\gamma I \end{bmatrix}.$$

* denotes a symmetric matrix element,

This article has been accepted for publication in IEEE Transactions on Intelligent Vehicles. This is the author's version which has not been fully edited and content may change prior to final publication. Citation information: DOI 10.1109/TIV.2023.3337863

$$\Xi_{\hat{R}} = \begin{bmatrix} \Pi(\tilde{R})+2\hat{R}_k & \tilde{R}_i\tilde{B}_{1_j} + \tilde{R}_j\tilde{B}_{1_i} & \tilde{C}_{1_i}{}^T + \tilde{C}_{1_j}{}^T \\ * & -2\gamma I & \tilde{D}_{11_i}^T + \tilde{D}_{11_j}^T \\ * & * & -2\gamma I \end{bmatrix},$$

$$\Xi_{\hat{S}} = \begin{bmatrix} \Pi(\tilde{S})-2\hat{S}_k & \tilde{S}_i\tilde{C}_{1_j}{}^T + \tilde{S}_j\tilde{C}_{1_i}{}^T & \tilde{B}_{1_i} + \tilde{B}_{1_j} \\ * & -2\gamma I & \tilde{D}_{11_i} + \tilde{D}_{11_j} \\ * & * & -2\gamma I \end{bmatrix},$$

$$\Pi(\tilde{R})=\tilde{A}_i^T\tilde{R}_j + \tilde{R}_j\tilde{A}_i + \tilde{A}_j^T\tilde{R}_i + \tilde{R}_i\tilde{A}_j, \tag{65}$$

$$\Pi(\tilde{S})=\tilde{A}_i\tilde{S}_j + \tilde{S}_j\tilde{A}_i^T + \tilde{A}_j\tilde{S}_i + \tilde{S}_i\tilde{A}_j^T. \tag{66}$$

Proof: The proof of Theorem 1 is shown in Appendix A.

A general design procedure of the FTTTC is summarized as follows:

Step 1) Design a baseline PDLF LPV controller u_{LPV} for the nominal system (3) without consideration of disturbances and faults to obtain satisfactory tracking performances and H_∞ index.

Step 2) Design a NN-DO to observe the disturbances online by selecting the desired gain $L_d(x)$ and weight matrix $\hat{W}$ of the NNs.

Step 3) Develop a fault estimator to estimate the faults online through choosing the estimator gain $L_f(x)$.

Step 4) Combine the baseline PDLF LPV control with the disturbance compensation and the fault tolerant control raised by the disturbance observer and fault estimator to formulate the composite control law.

Now consider the trajectory tracking control problem shown in Fig.2. A mixed-sensitivity loop-shaping method is applied to achieve small tracking error and suppress disturbance effect on output, and the mixed-sensitivity criterion is

$$\left\| \begin{matrix} W_p S \\ W_u KS \end{matrix} \right\|_\infty < 1 \tag{67}$$

where performance weighting function W_p and robustness weighting function W_u are hand-tuned until the desired objectives of the closed-loop system are achieved. K is the control gain, S denotes the system sensitivity function, The prefilter $W_{pre-filter}$ in Fig.2 is parameterized as

$$W_{pre-filter}(s) = \frac{\tau_f}{s+\tau_f}, \tag{68}$$

where $1/\tau_f$ denotes time constant of the filter.

After the affine LPV model, as Eq.(10), is augmented with the weighting functions, shown in (67)~(68), a pair of positive definite symmetric matrices ($R(\rho)$,$S(\rho)$) can be achieved by the PDLF design using Theorem 1.

D. Control allocation

Assumption 2. The input distribution matrix is assumed to be factorized as

$$B_2(\rho)=B_v B_u(\rho), \tag{69}$$

where $B_v \in \mathbb{R}^{n\times l}$ is a constant matrix with full column rank, and the time varying matrix $B_u(\rho) \in \mathbb{R}^{l\times m}$. Assume rank($B_u(\rho)$)=l < m for all $\rho \in \Theta$. In the nominal mode,

$$B_2(\rho)u=B_v \underbrace{B_u(\rho)u_{act}}_{v} = B_v v \tag{70}$$

According to the flying-wing aircraft configuration, see Fig.1, there are fifteen control surfaces of u_{act} to be allocated which meet

$$v = \begin{bmatrix} \mathbf{f}_C \\ \tau_C \end{bmatrix}_{6\times 1} = B_u(\rho)u_{act}, \tag{71}$$

$$B_u = \begin{bmatrix} 0 & B_{xf2} & B_{xf3} & & & \cdots & & B_{xf13} & B_{xf14} & 0 \\ B_{yf1} & 0 & 0 & B_{yf4} & 0 & \cdots & B_{yf12} & 0 & 0 & B_{yf15} \\ 0 & B_{zf2} & B_{zf3} & & & \cdots & & B_{zf13} & B_{zf14} & 0 \\ B_{lf1} & 0 & 0 & B_{lf4} & 0 & \cdots & B_{lf12} & 0 & 0 & B_{lf15} \\ 0 & B_{mf2} & B_{mf3} & & & \cdots & & B_{mf13} & B_{mf14} & 0 \\ B_{nf1} & 0 & 0 & B_{nf4} & 0 & \cdots & B_{nf12} & 0 & 0 & B_{nf15} \end{bmatrix} \tag{72}$$

where $\mathbf{f}_C$ and τ_C are virtual control forces and moments, see Fig.2, B_{ifj} denotes control effect parameter of the j^{th} flap, $i = x, y, z, l, m, n$. To get each control surface and thruster input of the practical engineering, a control allocation is suggested to solve (71) with following constraints:

$$\begin{aligned} \max(u_{act}(t-T)+\dot{u}_{\min}T, u_{\min}) &= \underline{u} \le u_{act} \le \overline{u} \\ &= \min(u_{act}(t-T)+\dot{u}_{\max}T, u_{\max}) \end{aligned} \tag{73}$$

where $\boldsymbol{u_{min}}$, $\boldsymbol{u_{max}}$ $\dot{u}_{\min}$ and $\dot{u}_{\max}$ denote lower and upper bounds of the actuator position and rotating rate, respectively. $\underline{u}$ and $\overline{u}$ are lower and upper bounds of the actuator inputs. T denotes sample period.

An Active Set (AS) based Weight Least Square (WLS) allocation method (see Fig.3) is studied to the above control allocation problem of (71) and (73) [25].

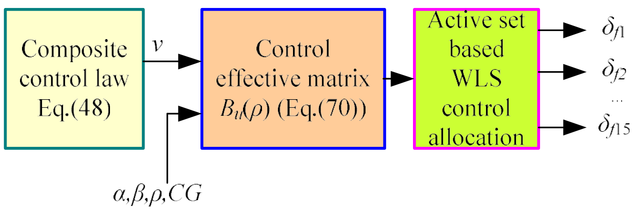

Fig. 3. Control allocation of the flying-wing aircraft

First find feasible solution set of the optimization problem

$$u_1 = \Omega = \arg\min_{\underline{u}\le u\le \overline{u}} \left\| W_v(B_u u_{act} - v)\right\|_2 \tag{74}$$

Second find the optimal solution that approaches the desired value $\boldsymbol{u}_d$

$$u^* = \arg\min_{u\in\Omega} \left\| W_u(u_{act} - u_d)\right\|_2 \tag{75}$$

where $\boldsymbol{W_u}$,$\boldsymbol{W_v}$ are the weighting matrix for prioritization of actuators and virtual control respectively. The 2-norm is

$\|u_{act}\|_2 = u_{act}^T u_{act}$. Ω denotes a feasible set. So the control allocation scheme of the FW aircraft is presented in Fig.3

By using the AS control allocation algorithm, the optimal inputs $\boldsymbol{u}^*$ are solved and each control allocation component is achieved and incorporated into the FTTTC scheme.

IV. Results and Discuss

To validate the proposed algorithm, a Cranfield University flying-wing aircraft is studied. The LPV model is derived by a small perturbation linearization method [2],where linearization is very simply accomplished by constraining the motion of the aeroplane to small perturbations about the trim condition. The considered model is a large flying-wing aircraft [16]. The initial state is as follows

$P_0 = [0, 0, 0]^T$(m), $\boldsymbol{V}_0 = [192 \text{ m/s}, 0, 0]^T$,

$\eta_0 = [0, 0.1, 0]^T$(rad), and $\omega_0 = [0, 0, 0]^T$,

where P_0 is position, V_0 is body velocity, η_0 is attitude and ω_0 is angular rate. Flight range is within $(u,h) \in ([167,218]) \times ([0,3048])$ (m/s, m). The actuator constraints are δ_e, δ_a, $\delta_r \in [-0.436, 0.436]$ (rad), and $\delta_p \in [0, 1]$. The state is $x_{lon}=[u\ w\ q\ \theta\ h]^T$, $x_{lat}=[v\ p\ r\ \ \phi\ \psi]^T$, the control is $u_{lon}=[\delta_e\ \delta_p]^T$, and $u_{lat}=[\delta_a\ \delta_r]^T$.

The LPV model as (1) , where

$$A(\rho) = A_0 + uA_u + hA_h \, , \tag{76}$$

$$B(\rho) = B_0 + uB_u + hB_h \, . \tag{77}$$

$$A_{0,\text{lat}} = \begin{bmatrix} 0.0022 & 24.1137 & -0.3993 & 9.7010 & 0 \\ -0.0056 & -0.4853 & 0.7759 & 0 & 0 \\ -0.0019 & -0.5035 & 0.0269 & 0 & 0 \\ 0 & 1.0000 & 0.1808 & 0 & 0 \\ 0 & 0 & 1.0108 & 0 & 0 \end{bmatrix},$$

$$A_{u,\text{lat}} = \begin{bmatrix} -0.0004 & -0.0538 & -1.0138 & 0.0004 & 0 \\ -0.0000 & -0.0201 & 0.0002 & 0 & 0 \\ 0.0000 & 0.0013 & -0.0009 & 0 & 0 \\ 0 & 0 & -0.0006 & 0 & 0 \\ 0 & 0 & -0.0000 & 0 & 0 \end{bmatrix},$$

$$A_{h,\text{lat}} = 1\times e^{-3} \begin{bmatrix} 0.0060 & 1.0744 & 0.2473 & -0.0070 & 0 \\ 0.0006 & 0.3561 & -0.0375 & 0 & 0 \\ -0.0001 & 0.0008 & 0.0142 & 0 & 0 \\ 0 & 0 & 0.0053 & 0 & 0 \\ 0.0052 & 0 & 0.0004 & 0 & 0 \end{bmatrix},$$

$$B_{0,\text{lat}} = \begin{bmatrix} 0.3066 & -1.6270 \\ 0.9725 & -0.3432 \\ -0.0145 & 0.1193 \\ 0 & 0 \\ 0 & 0 \end{bmatrix}, B_{u,\text{lat}} = \begin{bmatrix} -0.0038 & 0.0200 \\ -0.0120 & 0.0042 \\ 0.0002 & -0.0015 \\ 0 & 0 \\ 0 & 0 \end{bmatrix},$$

$$B_{h,\text{lat}} = 1\times e^{-3} \begin{bmatrix} 0.0339 & -0.1797 \\ 0.1074 & -0.0379 \\ -0.0016 & 0.0132 \\ 0 & 0 \\ 0 & 0 \end{bmatrix};$$

To achieve desired performances, the weight functions are chosen as follows,

$$W_{p_v} = \frac{0.1(0.5s+0.1827)}{s+0.001\times 0.1827} \; , W_{p_\psi} = \frac{0.7(0.5s+0.1827)}{s+0.001\times 0.1827},$$

and

$$W_{u_{\delta_a}} = \frac{2(s+0.1827/2)}{0.001s+0.1827} \; , W_{u_{\delta_r}} = \frac{4(s+0.1827/2)}{0.001s+0.1827},$$

$$W_{pre-filter}(s) = \text{diag}\left(\frac{500}{s+500}, \frac{500}{s+500}\right).$$

The longitudinal motion parameters $A_{0,\text{lon}}$, $A_{u,\text{lon}}$, $A_{h,\text{lon}}$, $B_{0,\text{lon}}$, $B_{u,\text{lon}}$, $B_{h,\text{lon}}$ and weight functions W_{p_u} , W_{p_h} , $W_{u_{\delta_p}}$, $W_{u_{\delta_e}}$ are the same as [16] .

Scenario I: trajectory tracking control for an LPV system under bounded disturbances $d(t)$.

Suppose the unknown harmonic disturbance vector d is as

$$d(t) = \left[0.05\sin(0.05t)(\text{rad}) \quad 0.1\cos(0.05t)\right]^T, \tag{78}$$

where $d(t)$ denotes $d_{lon} = \left[d_{\delta_e} \quad d_{\delta_p}\right]^T$ or $d_{lat} = \left[d_{\delta_a} \quad d_{\delta_r}\right]^T$. The weight matrices in Eq.(4) are

$$W_d = \begin{bmatrix} 0 & 0.05 \\ -0.05 & 0 \end{bmatrix}, \; V_{dlon} = \begin{bmatrix} 3.5 & 0 \\ 0 & 7 \end{bmatrix}, \; V_{dlat} = \begin{bmatrix} 0.04 & 0 \\ 0 & 2 \end{bmatrix},$$

The observer gains in (44) are designed as follows by section 3.B,

$L_{d\text{lon}}(x_{\text{lon}})$= [0 0 1e-4 0 0; 0.8e-4 0 0 0 0];

$L_{d\text{lat}}(x_{\text{lat}})$= [0 0.12 0 0 0; 0 0 0.012 0 0].

And the neural network parameters are selected as c= [-3 -2 -1 1 2 3; -3 -2 -1 1 2 3; -3 -2 -1 1 2 3; -3 -2 -1 1 2 3; -3 -2 -1 1 2 3;]; $h(0)$=[0.01,0.01,0.01,0.01,0.01,0.01]^T. γ_W= 1/0.1, b_j= 1.

To show the advantages of the proposed algorithm, an LPV synthesis control designed by Andrés Marcos *et al.* [11] is used for comparison, where the weight functions are chosen as follows

$$W_{ideal_H} = W_{ideal_v} = \frac{1}{s+1}, W_{ideal_V} = \frac{1}{8s+1}, W_{ideal_\phi} = \frac{1}{0.5s+1},$$

$$W_{p_H} = \frac{s/1.4+0.4}{s+0.004}, W_{p_V} = \frac{s/1.3+0.7}{s+0.007}, W_{p_v} = W_{p_\phi} = \frac{s/1.3+0.1}{s+0.1}$$

$$W_{\delta_e} = W_{\delta_a} = W_{\delta_r} = \frac{57.3}{25}, W_{\delta_p} = 1 \;,\; W_{noise_i} = \frac{s+0.4}{s+400} \; (i=1,2,3,4$$

This article has been accepted for publication in IEEE Transactions on Intelligent Vehicles. This is the author's version which has not been fully edited and content may change prior to final publication. Citation information: DOI 10.1109/TIV.2023.3337863

for each output),

and the lpvsyn function from MATLAB LPV Tools is used to obtain the LPV controller. The minimize index γ for the velocity, altitude and head angle tracking task by the LPV controller are achieved as follows

$$\gamma_V=0.7727, \quad \gamma_H=0.8836, \quad \gamma_\phi=0.9989,$$

To meet coordination turn requirement, β≈0, and the head angle tracking control is realized by using roll angle tracking control with $\dot{\psi} \approx g\sin\phi / V_0$, g is the gravity acceleration. The tracking responses by the LPV synthesis are Fig.4~ Fig.6.

Now according to **theorem 1,** the PDLF LPV design gain K_i (i = 1, 2, 3, 4) are achieved, and then the dynamic output feedback control of (5) is online calculated by using the convex combination (10) of the matrix vertices, and the performances obtained through the NNs-DO- PDLF approach are γ_{lon}= 1.01 and γ_{lat} = 2.36. By using the proposed controller, the forward velocity, altitude and head angle tracking responses of the flying-wing aircraft are given in Fig.4~ Fig.6.

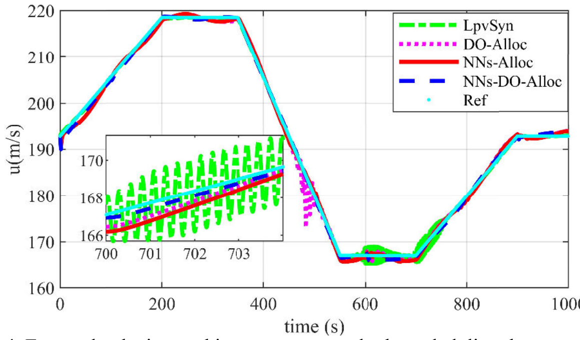

Fig.4. Forward velocity tracking responses under bounded disturbances

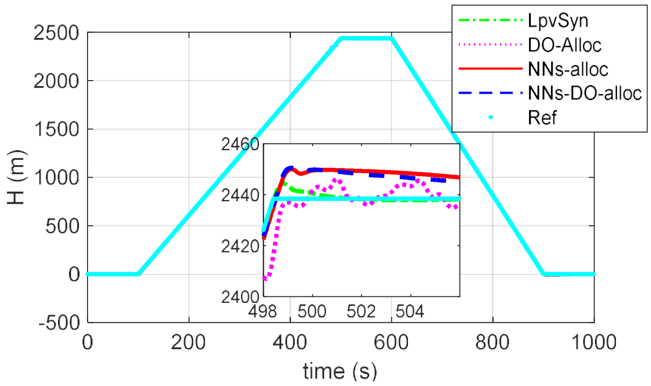

Fig. 5 Altitude tracking responses under bounded disturbances

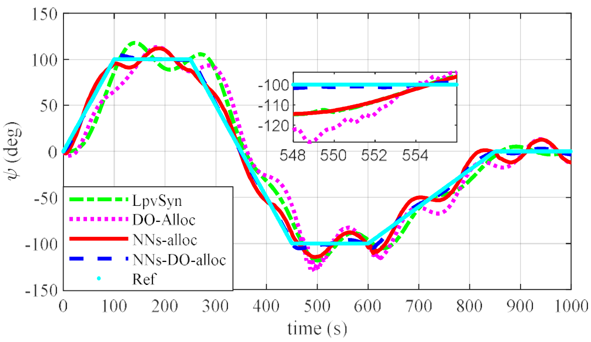

Fig. 6 Head angle tracking responses under bounded disturbances

Figs 4~6 show that the commanded forward velocity, altitude and head angle have been accurately tracked by the NNs-DO-PDLF LPV control. Compared with the conventional LPV synthesis design [11], DO – PDLF and NNs PDLF, there are smaller steady errors and lower overshoots than those for the NNs-DO-PDLF LPV design in speed and head angle tracking responses; Furthermore, there are some oscillations of LPV synthesis control in forward velocity and yaw angle tracking, which show that its tracking performances will deteriorate when large amplitude motion occurs following large disturbances, so the LPV synthesis has a bit vulnerability. Furthermore, there is large oscillation in altitude tracking response for the DO-PDLF with control allocation, but the response by the NNs-DO-PDLF control is quickly stable, this shows that the NNs- DO-PDLF design can reduce effect of observable disturbances and make their tracking responses more precise.

By the neural network observer the bounded observable disturbances are estimated as following.

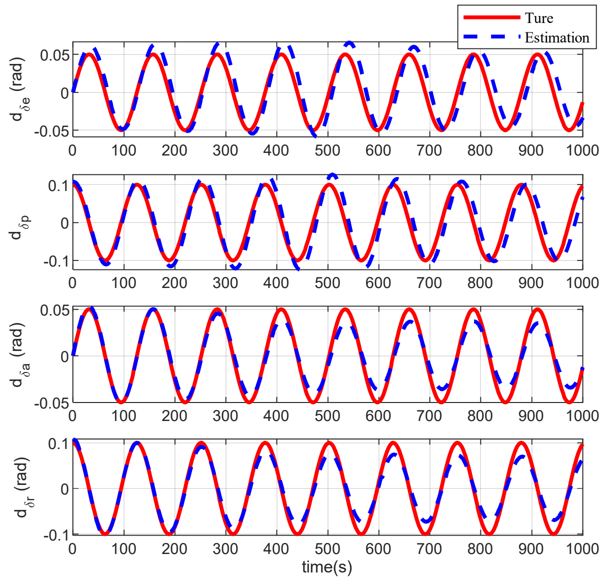

Fig. 7 Unknown observable disturbance estimation without control allocation

Fig.7 shows that estimation values of the disturbances approach to the true ones, but there is small deviation from the actual value, this is because the disturbance estimation $\hat{d}$ or $\hat{\xi}$ depends on the state as in (44), so it is easy affected by the state. But the small estimation errors are within the admissible range. Meanwhile, estimations of the harmonic frequency are the same as the original disturbances.

To show the effect of the weight vector of the RBF-NN in (42), we chose γ_w =1, γ_w =10 and γ_w =100 for comparison, and the simulation results are shown as follows

This article has been accepted for publication in IEEE Transactions on Intelligent Vehicles. This is the author's version which has not been fully edited and content may change prior to final publication. Citation information: DOI 10.1109/TIV.2023.3337863

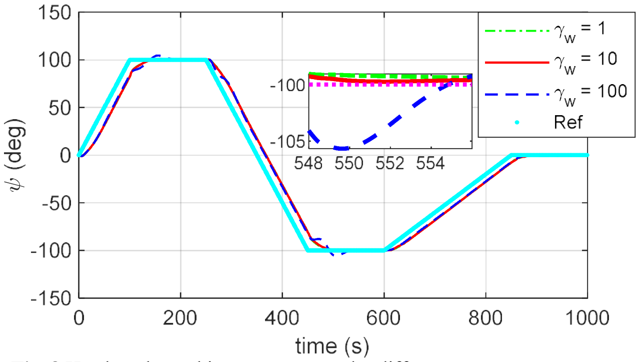

Fig. 8 Head angle tracking responses under different γ_w

From Fig.8 it can be seen that the head angle tracking precise will improve when the γ_w increases, but it will produce overshoot when γ_w is over large, so selecting suitable learning rate is important.

Scenario II: Fault tolerant tracking control for an LPV system with actuator faults.

Suppose the disturbance vector d is the same as Scenario I, and the unknown actuator fault vector f_a is

$$f_a(t) = \begin{cases} \begin{bmatrix} -0.0002t & 0.001t \end{bmatrix}^T, & t < 100 \\ \begin{bmatrix} -0.02 & 0.1 \end{bmatrix}^T, & t \geq 100 \end{cases} \quad (79)$$

where f_a are $f_{a,lon}(t) = \begin{bmatrix} f_{\delta_e} & f_{\delta_p} \end{bmatrix}^T$, $f_{a,lat}(t) = \begin{bmatrix} f_{\delta_a} & f_{\delta_r} \end{bmatrix}^T$ (rad). The gains of the fault observer (46) are obtained after several design iterations as follows,

$L_{flon}(x)$= [0 0 1.333e-4 0 0; 1.065e-4 0 0 0 0];

$L_{flat}(x)$= [0 0.015 0 0 0; 0 0 0.035 0 0].

According to **theorem 1,** the fault tolerant control gain K_i (i = 1, 2, 3, 4) and the associated dynamic controller are achieved. The output tracking responses are given as follows by using the proposed controller,

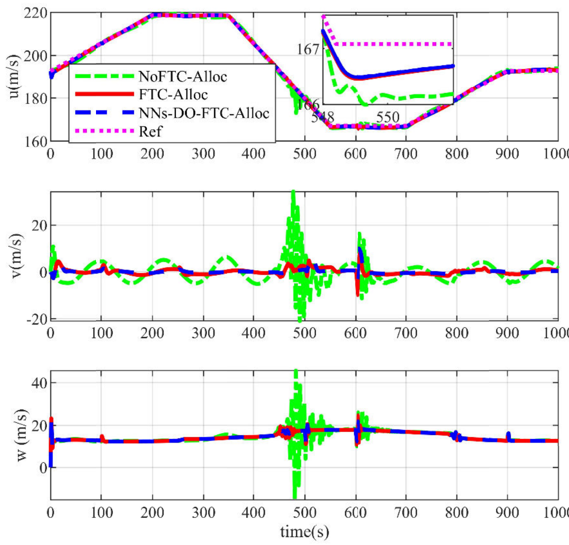

Fig. 9 Speed tracking output under actuator faults and disturbances

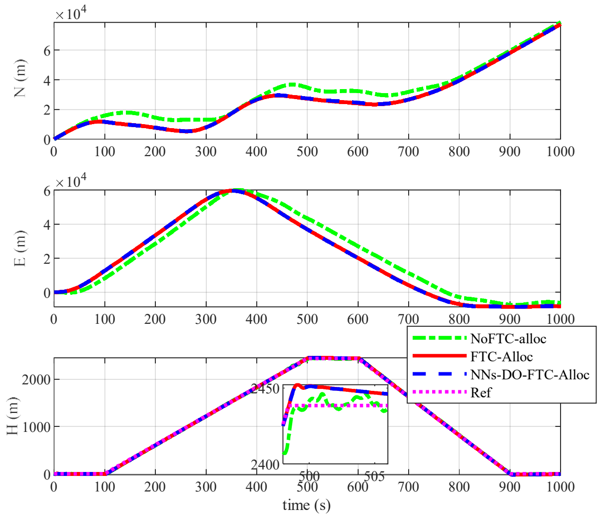

Fig.10 Position tracking output under actuator faults and disturbances

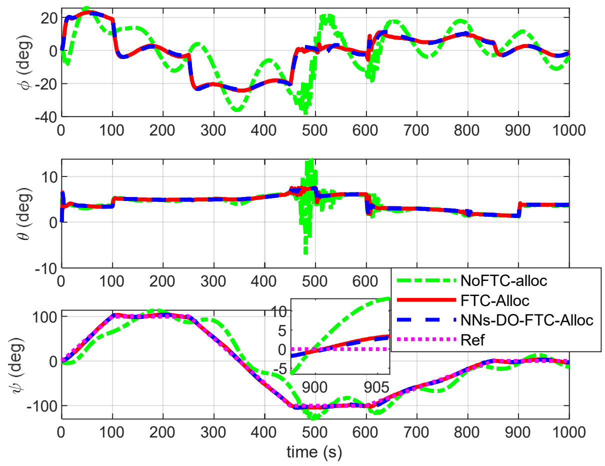

Fig.11 Attitude output responses under actuator faults and disturbances

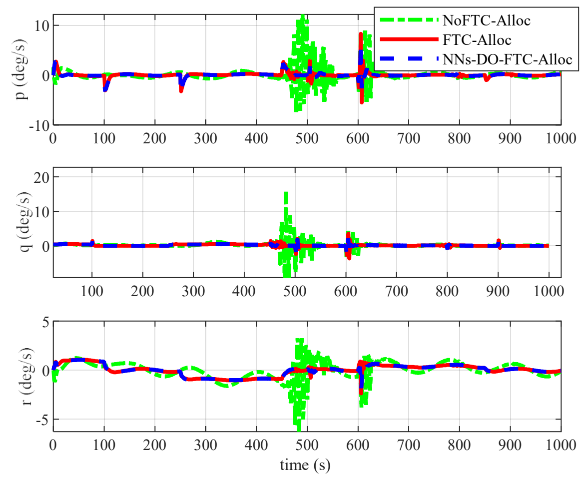

Fig.12 Angular rate output responses under actuator faults and disturbances

Figs 9~11 show that the reference signals of u_{ref}, h_{ref} and ψ_{ref} are precisely tracked by the NNs-DO-FTC design. Compared

This article has been accepted for publication in IEEE Transactions on Intelligent Vehicles. This is the author's version which has not been fully edited and content may change prior to final publication. Citation information: DOI 10.1109/TIV.2023.3337863

with PDLF control without fault tolerance, the FTTTC design has smaller steady errors and lower overshoots in the output responses of forward velocity, altitude and head angle. For the only PDLF control without FTC, there are big oscillations in the responses of speed, attitude and angular rates, which show worse control performances of the only PDLF at high altitude. This demonstrates the NNs-DO-PDLF LPV control not only has robustness in disturbance rejection, but also has strong fault tolerant capability. Comparison DO-PDLF FTC without NNs compensation, the tracking responses by the proposed NNs-DO-FTC are more approximate to the desired values, but this advantage is not obvious. The associated responses of the angular rates and control inputs are as in Fig.12 and Fig.13. Fig.12 shows that larger oscillations happen in the responses by the PDLF design without fault estimation than by the proposed FTC and NNs-FTC design. This is because the FTTTC compensates the fault effect by fault estimator. The control inputs of flaps 4, 12, left and right rudders are shown in Fig.13, the deflections of other flaps aren't listed here.

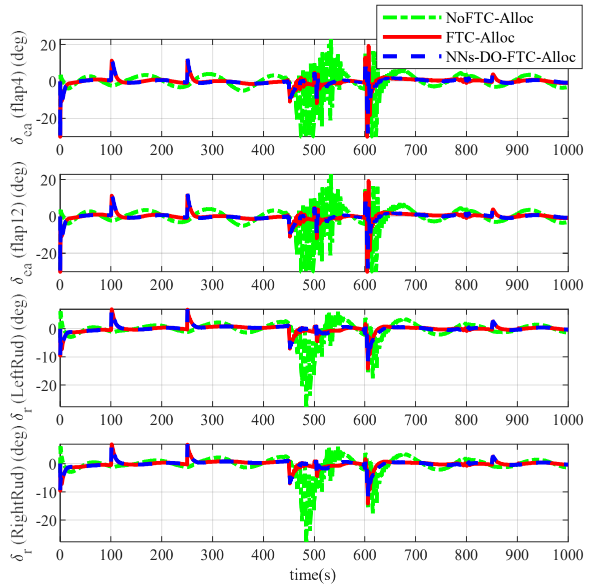

Fig.13 Inputs of flaps 4, 12 and rudders under Scenario II

From Figs 13, it can be seen that flaps 4, 12, left and right rudders are driven by the FTTTC with control allocation, which drives each control surface to improve control effectiveness and reduces saturation of each control surface.

The faults have been observed via fault estimation as in Figs 14, and the disturbances have also been observed via DOs, which are consistent with Fig.7.

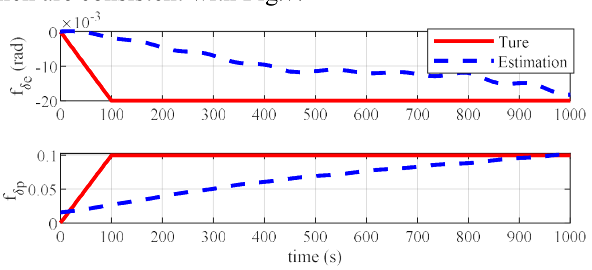

(*a*)

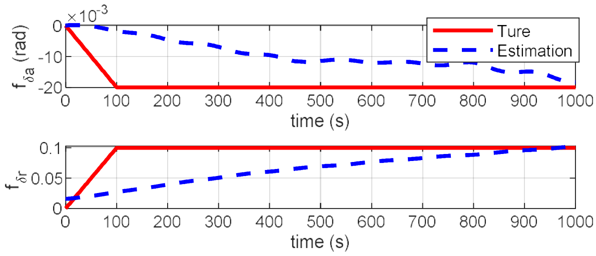

(*b*)

Fig.14 Unknown fault estimation with control allocation

Fig.14 shows that the estimations of actuator faults are asymptotically convergent to the true values, although some errors occur in the transition stage; this is because the fault estimation is changing with the associated states as (46).

V. Conclusion

This study achieves the fault tolerant trajectory tracking for a flying-wing aircraft with bounded disturbances and unknown actuator faults. A composite control scheme of the NNs-DO-PDLF LPV design is proposed. The trajectory tracking control for the LPV system is designed by a mixed-sensitivity loop-shaping method, thus the robust and tracking performance can be achieved simultaneously. To reduce conservatism of the LPV design, a PDLF LPV control is presented, and it can be easily obtained by the LMI technique.

To reduce the external disturbances an RBF neural network based observer is proposed and the disturbance rejection capabilities are improved. An LPV fault estimator is developed to estimate the actuator faults, and which is embedded into the composite controller to provide a fault tolerant function. Finally an active set based weight least square allocation method is presented to implement control allocation under actuator saturations. Simulation results of forward speed, altitude and head angle tracking control of the flying-wing aircraft validate the effectiveness of the proposed FTTTC design. It's shown that the FTTTC is able to accurately tracking the input commands even in with bounded disturbances and unknown faults. The problem that how to realize trajectory tracking under ice and other extreme condition is a new challenge for the FW aircraft, physics-informed data-based LPV modeling [28] and model-based reinforcement learning control [29] are promising methods for future work.

APPENDIX A

PROOF OF THEOREM 1

Proof: First the unknown disturbance $d(t)$ and actuator fault $f_a(t)$ are not considered. By Lemma 2, LMIs (33) are solvable for $\tilde{K}_i$ if and only if there exist a pair of positive definite symmetric matrices ($R(\rho)$, $S(\rho)$) defined in (30) satisfying

$$\sum_{i=1}^{r}\sum_{k=1}^{r}\alpha_i\alpha_i\beta_k\left(\bar{N}_R^T\Xi_R\bar{N}_R\right)+\sum_{i=1}^{r-1}\sum_{j=i+1}^{r}\sum_{k=1}^{r}\alpha_i\alpha_j\beta_k\left(\bar{N}_R^T\Xi_{\hat{R}}\bar{N}_R\right)<0 \tag{A1}$$

$$\sum_{i=1}^{r}\sum_{k=1}^{r}\alpha_i\alpha_i\beta_k\left(\bar{N}_S^T\Xi_S\bar{N}_S\right)+\sum_{i=1}^{r-1}\sum_{j=i+1}^{r}\sum_{k=1}^{r}\alpha_i\alpha_j\beta_k\left(\bar{N}_S^T\Xi_{\hat{S}}\bar{N}_S\right)<0$$

(A2)

$$\sum_{i=1}^{r} \alpha_i \begin{pmatrix} R_i & I \\ I & S_i \end{pmatrix} > 0, \quad (A3)$$

Note that (A3) ensures R_i, S_i >0 and $\left(R_i - S_i^{-1}\right) \geq 0$. By Lemma 1, (A1) ~ (A3) are sufficiently validated at all vertices if (59)~(64) are met. Furthermore, the lowest quadratic H_∞ index γ is achieved for both the ($R(\rho)$, S) and (R, $S(\rho)$) cases. Hence, the LPV controller u_{LPV} can stabilize the closed-loop system (6) by using the parameter dependent Lyapunov function $V(x)=x^T P(\rho)x$.

In order to stabilize the system for any disturbance $d(t)$ and any actuator fault $f_a(t)$, a part of the control effort, $v(x, d, f_a)$, shall linearly depend on the disturbance d and fault f_a. Thus, the control law can be divided into

$$v(x,d,f_a) = u_{LPV}(t) + K_d(x)d(t) + K_f(x)f_a(t) \quad (A4)$$

Substituting (A4) into the system (3) yields

$$\dot{x}(t) = A(\rho)x(t) + B_1(\rho)\omega(t) + B_2\left(u_{LPV}(t) + K_d(x)d(t) + f_a(t)\right) + B_3 d(t) \quad (A5)$$

Under condition that $B_3 = B_2$, $K_d(x) = -1$, and $K_f(x) = -1$, the closed-loop system reduces to

$$\dot{x}(t) = A(\rho)x(t) + B_1(\rho)\omega(t) + B_2 u_{LPV}(t) \quad (A6)$$

which is global exponentially stable under an appropriately designed controller (5). Since the external disturbance d and actuator fault f_{a} are unavailable, they are estimated by the disturbance observer (44) and fault estimator (46). Furthermore, because the observer gain $L_d(x)$ and $L_f(x)$ are appropriately determined such that $W_d - L_d(x)B_3V_d$ and $-L_f(x)B_2$ are Hurwitz respectively, the disturbance converges globally exponentially, and the fault estimator is globally exponentially stable [26]. After replacing the disturbance d and fault f_{a} by their estimations in the control law (A4), the closed-loop system (A5) becomes

$$\dot{x}(t) = A(\rho)x(t) + B_1(\rho)\omega(t) + B_2 u_{LPV}(t) + B_2\left(d(t) - \hat{d}(t)\right) + B_2\left(f_a(t) - \hat{f}(t)\right) \quad (A7)$$

Augmenting (A7) with the observer error dynamics (45) and (47) gives the closed-loop system under the composite controller, as

$$\begin{cases} \dot{x}(t) = A(\rho)x(t) + B_1(\rho)\omega(t) + B_2\left(u_{LPV}(t)\right) + B_2 e_d + B_2 e_f \\ \dot{e}_\xi(t) = \left(W_d - L_d(x)B_3V_d\right)e_\xi(t) - B_1(\rho)\omega \\ \dot{e}_f(t) = \dot{f}_a - \dot{\hat{f}}_a = -L_f(x)B_2 e_f(t) - B_3V_d e_\xi(t) - B_1(\rho)\omega + \dot{f}_a(t) \end{cases} \quad (A8)$$

where $e_d = V_d e_\xi$, $e_f = f_a(t) - \hat{f}(t)$. Because the system (A6) is exponentially stable, it implies that there exists the parameter dependent Lyapunov function

$$V_c(x) = x^T P(\rho)x,\ P(\rho) > 0. \quad (A9)$$

If there are positive definite symmetric matrix solutions ($R(\rho)$, $S(\rho)$) of the LMIs of (59)-(64), then we get

$$\frac{d}{dt}\left(V_c\right) + z^T z - \gamma\omega^T\omega < 0,\ \dot{V}_c(x) < -z^T z + \gamma\omega^T\omega, \quad (A10)$$

and $\|z\|_2 < \gamma\|\omega\|_2$, and $\dot{V}_c(x) < 0$. For the error dynamics of the disturbance observer, construct a Lyapunov function $V_o(e_\xi) = e_\xi^T P e_\xi$, then by using Lyapunov theory and it further follows from Theorem 1 in Ref.[16], we get

$$\dot{V}_o(e_\xi) < -\begin{pmatrix} z \\ e_\xi \end{pmatrix}^T \tilde{\Lambda}_d \begin{pmatrix} z \\ e_\xi \end{pmatrix}, \quad (A11)$$

where $\tilde{\Lambda}_d = \begin{bmatrix} \alpha_1^{-1}\gamma^{-1} & 0 \\ 0 & \kappa_o + \alpha_1 P B_1(\rho) B_1^T(\rho) P \end{bmatrix}$.

Therefore, the closed-loop system of (A8) with the NN-DO is exponentially stable, which implies that for an initial state x and ξ meeting $\| x(0) \| \leq \bar{x}_0$, $\| \xi(0) \| \leq \bar{\xi}_0$, and $\lim_{t\to\infty} x(t) \to 0$, $\lim_{t\to\infty} e_\xi(t) \to 0$, where $\bar{x}_0$ and $\bar{\xi}_0$ are given scalars.

Similarly, for the error dynamics of the fault estimation, we can obtain

$$\dot{V}_f(e_f) < -\begin{pmatrix} z \\ e_f \end{pmatrix}^T \tilde{\Lambda}_f \begin{pmatrix} z \\ e_f \end{pmatrix}, \quad (A12)$$

where $V_f(e_f) = e_f^T P e_f$ is a Lyapunov function candidate, $\tilde{\Lambda}_f$ is a small positive scalar as in $\tilde{\Lambda}_d$ in (A11).

For the nominal system of (A6) (without consideration of disturbance d and fault f_a), if the system is exponentially stable, then there exists a Lyapunov function $V_c(x)$ such that (56)~(58) are feasible for all $x \in \Xi_{r_0}$, $r_0 \leq r$[24]. Furthermore, when there exist disturbance d and fault f_a, since the observer gains $L_d(x)$ and $L_f(x)$ are appropriately chosen such that $W_d - L_d(x)B_3V_d$ and $-L_f(x)B_2$ are Hurwitz respectively, that is, the exponential stability of the disturbance observer and the fault estimator regardless of x, it implies that there exists a $k > 0$ and $\lambda > 0$ such that the trajectory of the observer error dynamic system satisfies

$$\|e_\xi(t)\| \leqslant k\|e_\xi(0)\|e^{-\lambda t},\ \forall e_\xi(0) \in \Xi_\sigma,\ x \in \Gamma,\ t \geqslant 0, \quad (A13)$$

where $\Xi_\sigma = \{e_\xi \in R^n, \mid \|e_\xi\| < \sigma_0\}$ with $\sigma_0 < \sigma/k$. It follows from Lemma 3 that there exist function $W_o(e_\xi, x)$ and $W_f(e_f, x)$: $\Xi_\sigma \times \Gamma \rightarrow R$ such that

$$\begin{aligned} & b_1\left\|e_\xi\right\|^2 \leq W_o(e_\xi, x) \leq b_2\left\|e_\xi\right\|^2 \\ & \frac{\partial W_o}{\partial x}\dot{e}_\xi \leq -b_3\left\|e_\xi\right\|^2 \\ & \left\|\frac{\partial W_o}{\partial e_\xi}\right\| \leq b_4\left\|e_\xi\right\|, \left\|\frac{\partial W_o}{\partial x}\right\| \leq b_5\left\|e_\xi\right\|^2 \end{aligned} \quad (A14)$$

for all $e_\xi \in \Xi_\sigma$. Define a Lyapunov function candidate $V_c(x,e_\xi)$ for the closed-loop system (A8) without faults as

$$\Phi(x,e_\xi)=V_c(x)+W_o(e_\xi,x) \quad \text{(A15)}$$

Taking the derivative of $V_c(x,e_\xi)$ along the trajectory of the closed-loop system (A8), one can obtain

$$\dot{\Phi}(x,e_\xi)=\frac{\partial V_c}{\partial x}\dot{x}+\frac{\partial W_o}{\partial x}\dot{x}+\frac{\partial W_o}{\partial e_\xi}\dot{e}_\xi$$

$$\le -c_3\|x\|^2+\left(\frac{\partial V_c}{\partial x}+\frac{\partial W_o}{\partial x}\right)B_2 e_\xi+\frac{\partial W_o}{\partial x}f_c-b_3\|e_\xi\|^2 \quad \text{(A16)}$$

where $f_c(x)=A(\rho)x(t)+B_1(\rho)\omega(t)+B_2u_{LPV}(t)$, $\bar{B}_1 \triangleq \max_{x\in\Xi_r}\|B_1(\rho)\|$, $\bar{B}_2 \triangleq \max_{x\in\Xi_r}\|B_2\|$. In addition, based on Eqs. (56)~(58), and (A14), we can obtain the following inequalities.

$$\left(\frac{\partial V_c}{\partial x}+\frac{\partial W_o}{\partial x}\right)B_2 e_\xi \le \left(\left\|\frac{\partial V_c}{\partial x}\right\|+\left\|\frac{\partial W_o}{\partial x}\right\|\right)\|B_2\|\cdot\|e_\xi\|$$

$$\le c_4\|x\|\bar{B}_2\|e_\xi\|+b_5\|e_\xi\|^3\bar{B}_2 \quad \text{(A17)}$$

$$\frac{\partial W_o}{\partial x}f_c(x)\le\left\|\frac{\partial W_o}{\partial x}\right\|\cdot\|f_c(x)\|\le b_5\|e_\xi\|^2\cdot l_3\|x\| \quad \text{(A18)}$$

where $l_3=\max_{x\in\Xi_r}\left\|\frac{\partial f_c(x)}{\partial x}\right\|$. Substituting (A17) ~ (A18) into (A16) yields

$$\dot{\Phi}(x,e_\xi)\le -c_3\|x\|^2+c_4\|x\|\bar{B}_2\|e_\xi\|$$

$$+b_5\|e_\xi\|^3\bar{B}_2+b_5\|e_\xi\|^2\cdot l_3\|x\|-b_3\|e_\xi\|^2 \quad \text{(A19)}$$

For all $e_\xi\in\Xi_\sigma$, $l_b\|e_\xi\|^2\cdot\|x\|\le\tilde{l}_b\|e_\xi\|\cdot\|x\|$, $b_5\|e_\xi\|^3\bar{B}_2\le\tilde{b}_5\|e_\xi\|^2\bar{B}_2$, where

$l_b=b_5\cdot l_3$, $\tilde{l}_b=l_b\sigma_0$, $\tilde{b}_5=b_5\sigma_0$, then (A19) satisfies

$$\dot{\Phi}(x,e_\xi)\le -c_3\|x\|^2+\left(c_4\bar{B}_2+\tilde{l}_b\right)\|e_\xi\|\cdot\|x\|+\left(\tilde{b}_5\bar{B}_2-b_3\right)\|e_\xi\|^2$$

$$\le-\frac{c_3}{2}\|x\|^2-\left(b_3-\tilde{b}_5\bar{B}_2-c_5\right)\|e_\xi\|^2 \quad \text{(A20)}$$

where $c_5=\left(c_4\bar{B}_2+\tilde{l}_b\right)^2/(2c_3)$. This implies that the exponential stability of the closed-loop system under the proposed controller is guaranteed by choosing a sufficiently large b_3 such that

$$b_3-\tilde{b}_5\bar{B}_2-c_5>0 \quad \text{(A21)}$$

Consider disturbances with simultaneous actuator faults, define the Lyapunov function candidate for the closed-loop system of (A8) as

$$\Phi(x,e_\xi,e_f)=V_c(x)+W_o(e_\xi,x)+W_f(e_f,x) \quad \text{(A22)}$$

one has

$$\dot{\Phi}(x,e_\xi,e_f)=\frac{\partial V_c}{\partial x}\dot{x}+\frac{\partial W_o}{\partial x}\dot{x}+\frac{\partial W_o}{\partial e_\xi}\dot{e}_\xi+\frac{\partial W_f}{\partial x}\dot{x}+\frac{\partial W_f}{\partial e_f}\dot{e}_f$$

$$\le -c_3\|x\|^2+\left(\frac{\partial V_c}{\partial x}+\frac{\partial W_o}{\partial x}+\frac{\partial W_f}{\partial x}\right)B_2e_\xi$$

$$+\frac{\partial W_o}{\partial x}f_c-b_3\|e_\xi\|^2+\frac{\partial W_f}{\partial x}f_c-a_3\|e_f\|^2$$

$$\le -c_3\|x\|^2+c_4\|x\|\bar{B}_2\|e_\xi\|+c_4\|x\|\bar{B}_2\|e_f\|+b_5\|e_\xi\|^3\bar{B}_2$$

$$+b_5\|e_\xi\|^2\cdot l_3\|x\|-b_3\|e_\xi\|^2+a_5\|e_f\|^3\bar{B}_2+a_5\|e_f\|^2\cdot l_4\|x\|-a_3\|e_f\|^2$$

$$\le -c_3\|x\|^2+\left(c_4\bar{B}_2+\tilde{l}_b\right)\|e_\xi\|\cdot\|x\|$$

$$+\left(c_4\bar{B}_2+\tilde{l}_{bf}\right)\|e_f\|\cdot\|x\|+\left(\tilde{b}_5\bar{B}_2-b_3\right)\|e_\xi\|^2+\left(\tilde{a}_5\bar{B}_2-a_3\right)\|e_f\|^2$$

$$\le -c_3\|x\|^2+\frac{c_3}{2}\|x\|^2+c_5\|e_\xi\|^2+\left(\tilde{b}_5\bar{B}_2-b_3\right)\|e_\xi\|^2$$

$$+\frac{c_3}{2}\|x\|^2+c_6\|e_f\|^2+\left(\tilde{a}_5\bar{B}_2-a_3\right)\|e_f\|^2$$

$$=-\left(b_3-\tilde{b}_5\bar{B}_2-c_5\right)\|e_\xi\|^2-\left(a_3-\tilde{a}_5\bar{B}_2-c_6\right)\|e_f\|^2 \quad \text{(A23)}$$

where a_i (i =1,2,…, 5), $\tilde{a}_5$ and $\tilde{l}_{bf}$ are positive constants defined the same as b_i, $\tilde{b}_5$ and $\tilde{l}_b$ in (A14),

$$c_6=\left(c_4\bar{B}_2+\tilde{l}_{bf}\right)^2/(2c_3). \quad \text{(A24)}$$

This means that selecting a sufficiently large b_3 and a_3 such that

$$b_3-\tilde{b}_5\bar{B}_2-c_5>0,\ a_3-\tilde{a}_5\bar{B}_2-c_6>0 \quad \text{(A25)}$$

then the exponential stability of the closed-loop system under the proposed controller is guaranteed. Hence, we can conclude that all the state, disturbance and fault estimate errors from a possible arbitrarily large set converges to the origin as $t\to\infty$. Therefore the results are achieved. □

REFERENCES

[1] M.Kozek, A.Schirrer, *Modeling and Control for a Blended Wing Body Aircraft-A Case Study*, Springer, Switzerland, 2015

[2] M. V. Cook and H. V.Castro, "The longitudinal flying qualities of a blended-wing-body civil transport aircraft", *The Aeronautical Journal*, Vol. 108, No. 1080, pp.75-84, 2004

[3] X. Xu, and Z. Zhou, "Study on longitudinal stability improvement of flying wing aircraft based on synthetic jet flow control", *Aerospace Science and Technology*, No.46, pp. 287-298, 2015

[4] A.Wildschek, "Flight Dynamics and Control Related Challenges for Design of a Commercial Blended Wing Body Aircraft", *AIAA Guidance, Navigation, and Control Conference*, AIAA SciTech Forum, National Harbor, Maryland, pp. 1-12. Jan. 2014

[5] H. Atoui, O. Sename, V. Milanes and J. J. Martinez, "LPV-Based Autonomous Vehicle Lateral Controllers: A Comparative Analysis", *IEEE Transactions on Intelligent Transportation Systems*, Vol.23, Issue8, 13570–13581. 2022

[6] P.M. Damon, D. Ichalal and H.Arioui, "Steering and Lateral Motorcycle Dynamics Estimation: Validation of Luenberger LPV Observer Approach", *IEEE Transactions on Intelligent Vehicles*, Vol.4, Issue 2 pp. 277-286, 2019

[7]Y.S. Quan, J.S. Kim, C.C. Chung, "Linear parameter varying models-based gain-scheduling control for lane keeping system with parameter reduction", *IEEE Transactions on Intelligent Transportation Systems*, Vol.23, Issue 11, 20746–20756. 2022

This article has been accepted for publication in IEEE Transactions on Intelligent Vehicles. This is the author's version which has not been fully edited and content may change prior to final publication. Citation information: DOI 10.1109/TIV.2023.3337863

[8] S.Q. Liu, Y.J. Sang, and H. B. Jin, "Robust model predictive control for stratospheric airships using LPV design", *Control Engineering Practice* , No.81, pp. 231-243, 2018

[9] M. Fleps-Dezasse, F.Svaricek, J. Brembeck,"Design and experimental assessment of an active fault-tolerant LPV vertical dynamics controller", *IEEE Transactions on Control Systems Technology* , Vol.27, No.3, pp. 1267-1274, 2019

[10] T.Y. He, A. K. Al-Jiboory, G.M. Zhu, S. S.-M. Swei, W.H. Su, "Application of ICC LPV control to a blended-wing-body airplane with guaranteed H_∞ performance", *Aerospace Science and Technology* , Vol. 81, pp. 88-98,2018

[11] A. Marcos, S. Waitman, M. Sato, "Fault tolerant linear parameter varying flight control design, verification and validation", *Journal of the Franklin Insti*tute,359, 653–676, 2022

[12] P.Apkarian and R.Adams. "Advanced gain-scheduling techniques for uncertain systems". *IEEE Transactions on Control Systems Technology* , Vol.6, No.1, pp. 21-32, 1998

[13] B. Shen, L. F. Xiao, and Z.F. Ye,. "Gain scheduling control of aero-engine based on mixing polynomial LPV synthesis", *International Journal of Turbo & Jet-Engines* , pp.1-12, 2023. https://doi.org/10.1515/tjj-2023-0001

[14]S. Chumalee, and J. F. Whidborne," Gain-scheduled $H\infty$ control via parameter-dependent Lyapunov functions", *International Journal of Systems Science* , Vol.46,No.1,pp. 125-138 ,2015

[15] S.Chumalee, and J. F.Whidborne, "Gain-scheduled $H\infty$ control for tensor product type polytopic plants", *Asian Journal of Control* , Vol.17, No.2, pp.417-431, 2015

[16] S.Q.Liu, J. F.Whidborne, S. Chumalee, "Disturbance observer enhanced neural network LPV Control for a Blended-wing-body large Aircraft", *IEEE Transactions on Aerospace and Electronic Systems* , Vol.57, No.5, pp. 2689-2703, 2021

[17] W. H. Chen, J. Yang, L. Guo, and S.H. Li, "Disturbance-Observer-Based Control and Related Methods—An Overview", *IEEE Transactions on Industrial Electronics* , Vol.63, No.2, pp. 1083-1095 , 2016

[18] S. H.Li, J.Yang, W.-H. Chen, X. S. Chen, *Disturbance Observer-Based Control- Methods and Applications* , CRC press, Taylor & Francis Group, Boca Raton, FL, pp.233-300, ch14, 2014

[19] Y.M. Li , Y. J. Liu , and S.C. Tong, "Observer-based neuro-adaptive optimized control of strict-Feedback nonlinear systems with state constraints", *IEEE Transactions on Neural Networks and Learning Systems* , Vol. 33, No. 7, pp.3131-3145, 2022

[20] K.Zhou, , J.Doyle, , and K.Glover, , *Robust and Optimal Control* , Englewood Clis, NJ: Prentice-Hall, 1995.

[21] P. C.Pellanda, P.Apkarian, and H. D.Tuan. "Missile autopilot design via a multi-channel LFT/LPV control method". *International Journal of Robust and Nonlinear Control* , 12, pp. 1-20, 2002

[22] S. Y.Cao, L.Guo, and X. Y. Wen, "Fault tolerant control with disturbance rejection and attenuation performance for systems with multiple disturbances", *Asian Journal of Control* , Vol.13,No.6, pp. 1056- 1064, 2011

[23] G.Herrmann, M. C.Turner, and I.Postlethwaite, Linear Matrix Inequalities in Control, in *Mathematical Methods for Robust and Nonlinear Control* : Springer-Verlag, Berlin Heidelberg, pp. 123-142, 2007

[24] H. K. Khalil, *Nonlinear systems* , 3rd ed. Prentice hall press, New Jersey. pp.366, 2002

[25] S.Q. Liu, S.J. Gong, Y.X. Li, Z.R. Lu. "Vectorial backstepping method based trajectory tracking control for an underactuted stratospheric airship", *The Aeronautical Journal* , 2017, 121(1241), 916-938.

[26] W. H.Chen, "Disturbance Observer Based Control for Nonlinear Systems", *IEEE/ASME Transactions on Mechatronics* , Vol.9, No.4, pp.706-710, 2004

[27] W. H. Chen, J. Yang, and Z. H. Zhao, "Robust control of uncertain nonlinear systems: a nonlinear DOBC approach". *Journal of Dynamic Systems, Measurement and Control* . Vol.138, No.7, 071002, pp. 1~9, 2016

[28] W. Wei, G. Yin and T. He, "Physics-Informed Data-Based LPV Modeling and Validations of Lateral Vehicle Dynamics," *IEEE Transactions on Intelligent Vehicles,* pp.1-10.2023, doi: 10.1109/TIV.2023.3303013.

[29] Z.K. Yao, X.L. Liang, G.P. Jiang,and J.Y. Yao, "Model-based reinforcement learning control of electrohydraulic position servo systems", IEEE/ASME Transactions on Mechatronics , Vol. 28, No. 3, 1446-1455, 2023

Shiqian Liu was born in Xinghua, Jiangsu Province, China. He received his MSc and PhD in Control Engineering from Nanjing University of Science and Technology (NUST), China. From 2005 to 2007 he was a postdoctoral research fellow in the national Key lab of Intelligent Technology and System, Tsinghua University. From 2019 to 2020 he is a visiting scholar in the School of Aerospace, Transport and Manufacturing, Cranfield University, United Kingdom. He is currently an associate professor in the School of Aeronautics and Astronautics, Shanghai Jiao Tong University. He serves as an associate editor of IEEE Transactions on Intelligent Vehicles. He has the author of two books, more than 70 articles, more than 8 inventions. His research interests are in the intelligent flight control, Vehicle dynamics and control, fault tolerant control, and UAVs.

Weizhi Lyu received his B.Eng. degree in Automation from Anhui University, Hefei, China, in2018 and his M.Sc degree in Control Science and Engineering from Beijing Institute of Technology, Beijing, China, in 2021. He is currently pursuing his Ph.D. degree in Aeronautical and Astronautical Science and Technology from Shanghai Jiao Tong University, Shanghai, China. His research interests include nonlinear control, adaptive control, flight control, linear parameter varying control.

Congjie Yang received his B.Eng. degree in Detection Guidance and Control Technology from Xidian University, Shanxi, China, in 2018 and is currently pursuing his Ph.D. degree in Aeronautical and Astronautical Science and Technology from Shanghai Jiao Tong University, Shanghai, China. His research interests include modeling of flexible aircraft and controller designing based on model.

Fei-Yue Wang (S'87-M'89-SM'94-F'03) received his Ph.D. in Computer and Systems Engineering from Rensselaer Polytechnic Institute, Troy, New York in 1990. In 1999, he founded the Intelligent Control and Systems Engineering Center at the Institute of Automation, Chinese Academy of Sciences (CAS), Beijing, China, under the support of the Outstanding Overseas Chinese Talents Program from the State Planning Council and "100 Talent Program" from CAS, and in 2002, was appointed as the Director of the Key Lab of Complex Systems and Intelligence Science, CAS. From 2006 to 2010, he was Vice President for Research, Education, and Academic Exchanges at the Institute of Automation, CAS. In 2011, he became the State Specially Appointed Expert and the Director of the State Key Laboratory for Management and Control of Complex Systems. His current research focuses on methods and applications for parallel systems, social computing, parallel intelligence and knowledge automation.

James F. Whidborne received his BA in engineering from the Cambridge University, United Kingdom, and MSc and PhD in systems and control from the University of Manchester Institute of Science and Technology (UMIST), United Kingdom. He is currently the Head of the Dynamics Simulation and Control Group in the Department of Aerospace Engineering at Cranfield University, United Kingdom. He has about 180 refereed research publications, including three books. He is a Chartered Engineer, a Member of the IET and a Senior Member of the IEEE. His research interests are in the theory and application of advanced control, including multiobjective robust control, fluid flow control, finite precision controller implementation problems and flight control problems.

2023-11-30

Neural network observer based LPV fault tolerant control of a flying-wing aircraft

Liu, Shiqian

IEEE